JOURNAL OF GEOPHYSICAL RESEARCH, VOL. 102, NO. D6, PAGES 6775–6797, MARCH 27, 1997

Numerical advection schemes, cross-isentropic random walks, and correlations between chemical species

John Thuburn
Centre for Global Atmospheric Modelling, Department of Meteorology, University of Reading, Reading, England

Michael E. McIntyre
Centre for Atmospheric Science at the Department of Applied Mathematics and Theoretical Physics, University of Cambridge, Cambridge, England

Abstract. The advection schemes used in numerical models of chemistry and transport at fixed resolution must unavoidably cause the models to misrepresent the transport in some way. This can include failure to establish or preserve the functional relations between long-lived chemical tracers that are often observed in the atmosphere. We show that linear functional relations will be preserved exactly by purely linear advection schemes and also, less obviously, by certain "semi-linear" flux-limited schemes despite the unavoidable nonlinearity introduced by the flux limiter. In practice, semi-linear flux-limited schemes will also preserve nonlinear functional relations better than linear centered difference or spectral schemes that suffer from dispersion errors. The reason is that the dispersion errors lead to spurious oscillations of the mixing ratio field in physical space, artificially expanding the range of mixing ratios in any neighborhood, and hence to a spurious scatter in the relation between any two mixing ratio fields that are nonlinearly related to begin with. Examples of correlations not only preserved, but established, by real and model transport are discussed in this light, including the case of stratospheric transport on timescales of years, for which we discuss and extend earlier results on the ways in which tracer functional relations can arise, for sufficiently long-lived tracers, purely from transport. The stratospheric results are shown not to depend on the quasi-horizontal Fickian eddy diffusivity assumption used in the earlier work. The reason is that, whenever the quasi-horizontal (isentropic) mixing is fast enough—even if it is non-Fickian as expected in real stratospheric surf zones—the chaotic part of the quasi-vertical, cross-isentropic transport has the nature of a random walk with small vertical steps.

1. Introduction

There has been much interest in the striking correlations, verging on functional relations, observed in the lower stratosphere between the mixing ratios of certain long-lived tracer species, or families of species, such as nitrous oxide (N_2O) and "total odd nitrogen" (NO_y) [e.g., *Fahey et al.*, 1990]. These correlations put observational constraints on attempts to model the atmosphere, and in particular they have emphasized shortcomings in advection schemes used for gas-phase transport in numerical models [e.g., *Allen et al.*, 1991]. This in turn has directed attention to fundamental differences between chemical transport in the real atmosphere and chemical transport in numerical models. All these issues have acquired new urgency in view of, for instance, recent controversies about observed correlations between N_2O and ozone (O_3) in the Arctic polar vortex. There is concern about whether the correlations are adequately represented in numerical models and whether departures from a simple functional relation between the species may or may not be interpreted as evidence for anomalous chemistry [e.g., *Proffitt et al.*, 1990, 1992; *McIntyre*, 1992; *Plumb and Ko*, 1992 (hereafter PK)].

If one chemical species is a source for another, if two species react together to destroy each other, or if two species are created together from other species, then the mixing ratios ψ and χ of the two species may be functionally related, with the function linear in the sense that

$$\chi = A\psi + B \tag{1}$$

Paper number 96JD03514.
0148-0227/97/96JD-03514$09.00

where A and B are constants. Moreover, such a relation is preserved by any mixing process. These considerations may have relevance, for instance, to the observed N_2O, NO_y relation [*Fahey et al.*, 1990]. However, as was recognized by *Fahey et al.* and examined in detail by PK, functional relations can arise for a different reason. Even when the chemistry is less simple, transport by itself can give rise to functional relations between species. This is especially liable to happen when chemical timescales are long in comparison with transport timescales. More generally, if two gas-phase species have common sources and sinks, and if the transport is the same for both species—these notions will be made precise below—then a functional relation can arise essentially because the transport shapes the ψ and χ fields in the same way, making their isopleths coincide [*Plumb and McConalogue*, 1988 (hereafter PM)].

This paper examines from a fundamental viewpoint the questions thus raised. First, we briefly recall why, for the real atmosphere, it often makes sense to talk about "the" transport, that is, a unique transport, the same for different gas-phase species. Second, we point out that no such uniqueness property holds, in any general sense, for numerical models at finite resolution, because of the nature of practical numerical advection schemes. Third, we show that, nevertheless, certain flux-limited advection schemes that are "semi-linear"—in a sense to be made precise—will exactly preserve preexisting linear functional relations between species, and will usually preserve preexisting nonlinear functional relations more accurately than do linear centered difference schemes with or without negative-value filling. Fourth, we reexamine the results of PM and PK concerning the ability of transport to establish, as well as to preserve, functional relations between species. PK's results on vertical diffusive behavior in the stratosphere and their predecessors in *Mahlman et al.* [1986] and *Holton* [1986] are generalized so as not to depend (*a*) on steadiness and zonal symmetry of the diabatic circulation and (*b*) on assuming Fickian quasi-horizontal eddy diffusivity. This generalization, equation (40) below, is important if only because the quasi-horizontal eddy diffusivity assumption is not well justified in, for example, real stratospheric surf zones. Fifth and finally, we discuss to what extent these results are likely to remain valid in numerical models using typical advection schemes, and to what extent we can expect numerical models, as distinct from the real atmosphere, to preserve preexisting functional relations between species or to establish such relations.

While focusing on fundamentals we nevertheless recognize that practical models with limited resolution may need to parameterize subgrid chemistry, and that such parameterizations will tend to blur the distinction between transport and chemistry, as with so-called "chemical eddy" effects. However, for the sake of conceptual clarity it is still worth maintaining, in principle, the distinction between transport and chemistry, and regarding their subgrid interactions as a separate parameterization problem distinct from the problems discussed here. The distinction between transport and chemistry is important, if only because it implies the possibility of thought experiments in which we keep the transport unchanged while changing the chemistry, and vice versa.

2. Linearity and Other Basic Properties of Real Gas-Phase Transport

For well-known reasons, gas-phase material transport in the real atmosphere is almost exactly independent of the thing transported, so that one can speak of "the" transport, the same for all gas-phase species. The only differences come from the finest, Kolmogorov-scale details of small-scale turbulent mixing, which depend on molecular diffusivity coefficients; but such differences are many orders of magnitude smaller than are likely to be significant in the present state of knowledge, and we disregard them from the outset.

The species-independence of gas-phase transport, together with the additivity property of conservable or transportable quantities, implies a certain "linearity property," namely, that the net effect of transport is representable mathematically as a linear operation on the mixing ratio fields ψ, χ, ... of gas-phase species. This linear operation is independent of the mixing ratio fields and dependent only on the air motion, including small-scale turbulent mixing. It can be expressed in various ways, of which the three best known take the form, in the absence of chemical sources and sinks,

$$\frac{\partial}{\partial t}(\rho\chi) = -\nabla.\mathbf{F}(\chi) \tag{2}$$

$$\frac{\partial \chi}{\partial t} = -L(\chi) \tag{3}$$

$$\chi(\mathbf{x},t) = \int R(\mathbf{x},\mathbf{x}';t,t')\chi(\mathbf{x}',t')\rho(\mathbf{x}',t')\,d^3\mathbf{x}' \quad (t \geq t') \tag{4}$$

[e.g., *Pasquill and Smith*, 1983; *Fiedler*, 1984; *Stull*, 1984; PM]. In (2) and (4), ρ is the air density, and $\mathbf{F}(\chi)$ is the total, advective plus nonadvective, flux or transport of the species whose mixing ratio is χ; $\mathbf{x}$ is position and t is time. In (3), $L(\chi)$ is the linear operator

$$L(\chi) = \mathbf{u}.\nabla\chi + \rho^{-1}\nabla.\{\mathbf{F}(\chi) - \rho\mathbf{u}\chi\} \tag{5}$$

The linearity property says that the flux vector $\mathbf{F}(.)$, hence its divergence, hence $L(.)$, depend linearly on their arguments, which implies that

$$\mathbf{F}(A\psi + B\chi) = A\mathbf{F}(\psi) + B\mathbf{F}(\chi) \tag{6}$$

for any constants A and B, and that

$$L(A\psi + B\chi) = A\,L(\psi) + BL(\chi) \tag{7}$$

Also, we normally assume that $L(A) = 0$, i.e., that transport cannot change any χ field that is spatially

uniform. In (4) the Green's function or redistribution function $R(\mathbf{x}, \mathbf{x}'; t, t')$, defined for $t \geq t'$, describes the transport taking place between times t' and t; the restriction $t \geq t'$ is needed, in general, because of the irreversibility of mixing. The linearity property says that R is independent of χ.

The linearity property reminds us why the notion of "eddy diffusivity" is usually ill defined for the real atmosphere. Although, for a single tracer species whose mixing ratio is χ, one can define a local, Fickian scalar or tensor eddy diffusivity K by forcing it to satisfy

$$\mathbf{F}(\chi) - \rho \mathbf{u} \chi = -\rho K \nabla \chi, \tag{8}$$

such a K will usually depend on the χ field. It may do so very strongly, as is well illustrated by the examples of linear passive tracer transport given by *Fiedler and Moeng* [1985]. In other words, linear transport can give nonlinear K, and different K for different species. This can happen—even in the absence of further complications, such as unresolved linear or nonlinear "chemical eddy" effects—because the statistically nonlocal character of real turbulent transport may conflict with the assumed local character of Fickian diffusion. In a coarse-grain, averaged description, which we must resort to unless we use space and time resolutions comparable to the Kolmogorov scales, an impracticable proposition, the averaged transport is linear but often non-Fickian—and statistically nonlocal—as with a random walk whose step size is not small in comparison with spatial scales of the averaged tracer fields. Real stratospheric surf zones, with their large horizontal eddy sizes, provide a conspicuous example. In (4) the redistribution function $R(\mathbf{x}, \mathbf{x}'; t, t')$ makes this nonlocalness explicit; *Stull* [1984] calls it "transilience."

As regards the advective contribution to $\mathbf{F}(\chi)$ namely $\rho \mathbf{u} \chi$, it might be thought that the linearity property expressed by (2), (3), or (4) could be straightforwardly represented in numerical models simply by using a linear advection scheme. But such schemes lead to well-known difficulties. For instance, linear schemes based on centered differences or on spectral transforms can generate spurious oscillations in the advected quantity, and even negative mixing ratios. Negative values are then "filled" in some way (set to zero or to a small positive value) and the tracer field is adjusted elsewhere to conserve the total mass of tracer substance. The scheme as a whole, advection plus filling, is nonlinear. Again, flux-limited advection schemes, which are currently fashionable because they can be designed to overcome the more conspicuous problems such as spurious production of negatives, are also nonlinear, intrinsically and unavoidably. In either case the linearity property is violated: the transport operator corresponding to the numerical scheme is not independent of the thing transported. The only linear schemes that do not require negative-value filling, namely, first-order upwind schemes [*Godunov*, 1959], do have the linearity property but are too diffusive for practical purposes.

In summary, then, no real transport situation can be perfectly represented in a practicable numerical model with fixed spatial resolution relying on an Eulerian advection scheme; one must have at least one of the following three problems: (*a*) spurious oscillatory behavior, including negative mixing ratios, as with linear centered difference schemes, (*b*) excessive linear diffusion, as with linear first-order upwind schemes, or (*c*) artificial nonlinearity, in the sense of artificial dependence of the transport on the thing transported, as with flux-limited schemes and, equally, linear schemes followed by negative-value filling. Because both problem (*a*) and problem (*b*) are intolerable in practice, we are left with problem (*c*), hence violation of the fundamental linearity property. One must therefore ask to what extent a flux-limited or any other nonlinear advection scheme will disrupt functional relations between tracer species or exhibit other departures from real atmospheric behavior, making model results difficult to interpret and difficult to compare with observations.

What other properties of real gas-phase transport need consideration? The following list of properties, some of which have been mentioned already, could be taken to be the most fundamental: **1**, the transport operator is linear, **2**, the total mass of tracer substance is conserved, **3**, absolute mixing ratio extrema are never amplified (absolute maxima are never increased nor absolute minima decreased), **4**, a spatially homogeneous mixing ratio field always remains spatially homogeneous, with the same mixing ratio value, and **5**, negative mixing ratios are never produced. Property **3** is sometimes called the "shape-preserving" property. If, in addition, the transport is purely advective then we have another property, **6**, all functional relations between different advected species are preserved.

Not all these properties are logically independent. For instance, property **3** implies properties **4** and **5** as special cases. Furthermore, properties **1**, **4**, and **5** together imply property **3**. This will be shown shortly. Note also that for any transport operator, real or numerical, that has property **3** and sees only a neighborhood of limited size—as with, for instance, a shape-preserving finite-difference scheme acting over a single timestep—property **3** will apply also to relative extrema within the neighborhood, because such a transport operator cannot distinguish relative extrema within the neighborhood from absolute extrema over the whole domain. This fact will be made use of in section 4.2.

For real gas-phase transport, properties **1**–**6** can be expressed via the redistribution function $R(\mathbf{x}, \mathbf{x}'; t, t')$. Property **1** holds whenever $R(\mathbf{x}, \mathbf{x}'; t, t')$ is independent of χ, as pointed out below equation (4). Property **2** will hold if and only if

$$\int R(\mathbf{x}, \mathbf{x}'; t, t')\, \rho(\mathbf{x}, t)\, d^3\mathbf{x} = 1 \quad \text{for all } \mathbf{x}',\ t' \leq t \tag{9}$$

(multiply equation (4) by $\rho(\mathbf{x}, t)$, integrate with respect to $\mathbf{x}$, and require the result to equal the given mass M

for all $\rho(\mathbf{x}',t')\chi(\mathbf{x}',t')$ having $\int \rho(\mathbf{x}',t')\chi(\mathbf{x}',t')d^3\mathbf{x}' = M$; compare equation (9) of *Fiedler* [1984] and (4) of *Stull* [1984]). It is straightforward to make an advection scheme satisfy property **2**, by basing it on the flux form, cf. equation (2), of the differential equation describing advection. Property **4** will hold if and only if

$$\int R(\mathbf{x},\mathbf{x}';t,t')\,\rho(\mathbf{x}',t')\,d^3\mathbf{x}' = 1 \quad \text{for all } \mathbf{x},\ t \geq t' \tag{10}$$

(immediately from equation (4); compare equation (7) of *Fiedler* [1984] and (3) of *Stull* [1984]). When based on the advective form, cf. equation (3), of the tracer advection equation, most schemes trivially satisfy property **4**. However, when the flux form is used, a certain cancellation is required between contributions to the flux divergence, consistent with mass continuity. Property **5** will hold if and only if

$$R(\mathbf{x},\mathbf{x}';t,t') \geq 0 \quad \text{for all } \mathbf{x},\ \mathbf{x}',\ t \geq t' \tag{11}$$

Many simple numerical transport schemes violate property **5**. Property **3** can now be seen to be implied, as already asserted, whenever properties **1**, **4**, and **5** all hold. For, if $\chi_{\max}(t') \geq 0$ and $\chi_{\min}(t') \geq 0$ are respectively the absolute maximum and minimum values of χ at time t', then to deduce property **3** we need only show that if χ evolves via (4) then $\chi(\mathbf{x},t) \leq \chi_{\max}(t')$ and $\chi(\mathbf{x},t) \geq \chi_{\min}(t')$, for any t and t' such that $t \geq t'$. But if χ evolves via (4) then so also do $\chi^{(1)}(\mathbf{x},t) = \chi_{\max}(t') - \chi(\mathbf{x},t)$ and $\chi^{(2)}(\mathbf{x},t) = \chi(\mathbf{x},t) - \chi_{\min}(t')$, as can be verified by substitution into the right of (4) followed by use of (10); and, because $\chi^{(1)}(\mathbf{x},t') \geq 0$ for any t', (4) and (11) together imply that $\chi^{(1)}(\mathbf{x},t) \geq 0$ for any $t \geq t'$, similarly $\chi^{(2)}(\mathbf{x},t) \geq 0$, and property **3** follows.

Property **3** does not, however, follow from properties **4** and **5** alone, and so it needs separate consideration for any practical, nonlinear, numerical transport scheme. Though property **3** is usually insisted on, we remark that cases are conceivable in which it would not be appropriate. A coarse-grain, averaged picture of real turbulent transport could violate property **3**, and **4** also. Coarse-grain χ fields may correspond to finer-grain χ fields having, say, larger maxima that are hidden by spatial or ensemble averaging. These could amplify a maximum in the coarse-grain χ field if unresolved fluid dynamical processes like subgrid-scale vortex merging take place. However, for conceptual clarity it is probably best to parameterize such effects separately and explicitly, if they are thought to be important, while retaining property **3** in the advection scheme. Many advection schemes that satisfy property **3** have been developed, based on the techniques of "flux-corrected transport" [e.g., *Boris and Book*, 1972; *Zalesak*, 1979] or of "flux limiters" [e.g., *Sweby*, 1985; *Leonard*, 1991; *Thuburn*, 1996], again at the cost of violating the linearity property.

That linear transport preserves linear functional relations is obvious from equation (4), by substituting (1) into the right hand side of (4). However, arbitrary functional relations between species will be preserved (property **6**) only if R corresponds to pure advection,

$$R(\mathbf{x},\mathbf{x}';t,t') = \frac{1}{\rho(\mathbf{x}',t')}\delta^3(\mathbf{x}' - \mathbf{X}(\mathbf{x},t,t')) \tag{12}$$

for some single-valued function $\mathbf{X}(\mathbf{x},t,t')$, the Lagrangian inverse map giving the departure point for a material particle subsequently at $\mathbf{x}$, where δ^3 is the three-dimensional Dirac delta function and $\rho(\mathbf{x}',t')$ is the air density at the departure point. Diffusion is not allowed here, even when the diffusion coefficient is the same for all species. Any diffusion or other mixing process acting on two air parcels having mixing ratio values $\chi = \chi_1$ and $\chi = \chi_2$ of one tracer will produce a range of mixing ratios along the "mixing line" defined by

$$\lambda\chi_1 + \mu\chi_2 \quad (0 \leq \lambda \leq 1,\ \ \mu = 1 - \lambda) \tag{13}$$

and similarly for a second tracer. So if two tracers are functionally related, as illustrated by the curve in Figure 1a, then mixing will tend to replace the functional relation by a scatter, by linearly interpolating along the mixing lines between pairs of points such as A and B or A and C. Clear examples of the formation of such mixing lines have been observed, for instance, during polar vortex breakup [e.g., *Waugh et al.*, 1996].

3. Examples of Advection Schemes

Three one-dimensional advection schemes are considered in this paper: (*a*) a second-order centered difference scheme (CD2), (*b*) a simple flux-limited scheme based on second-order differences plus the *van Leer* [1974] limiter (VL2), and (*c*) a more sophisticated flux-limited scheme (UL4) based on fourth-order centered differences plus a flux limiter equivalent to *Leonard*'s [1991] universal limiter. These three schemes are currently available as options for calculating the vertical advection terms in the UK Universities Global Atmospheric Modelling Programme (UGAMP) global circulation model (the UGCM; see, for example, *Slingo et al.* [1994]). Details are given in Appendix A below. *Thuburn* [1996] shows how the principles involved can be extended to more than one dimension and to arbitrary orders of accuracy.

All three schemes conserve the total mass of tracer substance, property **2** of section 2, listed above equation (9), and preserve an initially homogeneous mixing ratio, property **4**. CD2 is typical of advection schemes using centered differences in that dispersion errors lead to the production of spurious extrema, including negative tracer mixing ratios. VL2 and UL4, on the other hand, are shape preserving (property **3**) and produce no spurious extrema.

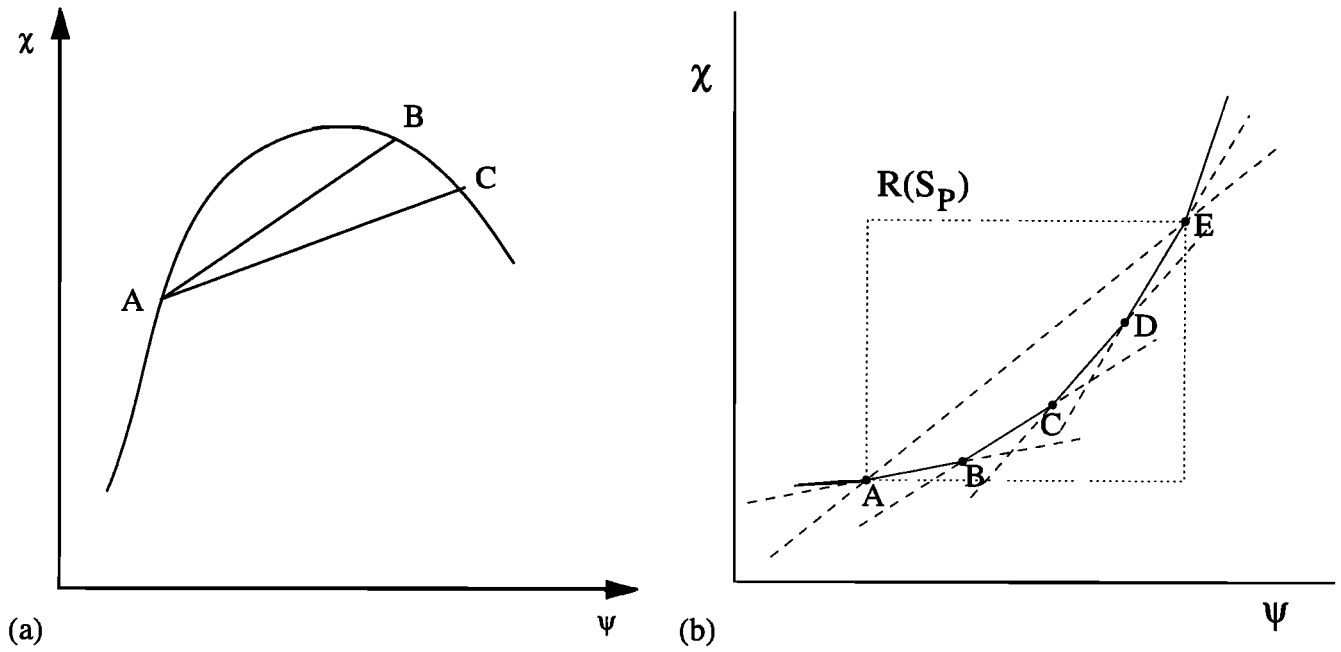

Figure 1. (a) Illustration of how the mixing of two species initially having a simple nonlinear functional relation (curved line) in a correlation diagram ($\psi\chi$ diagram), can disrupt that simple relation by generating new values along mixing lines, such as the straight lines shown. (b) Points A,B,...,E on a correlation diagram representing the relevant grid values of the mixing ratios ψ and χ of two species that initially satisfy a functional relation. The relevant grid values are those belonging to the set S_P of grid points seen by a numerical advection scheme, when updating mixing ratio values at the grid point P (see text). (The number of grid points of S_P, hence the number of points on the correlation diagram, is finite but may differ from the number shown schematically.) For a scheme that is shape preserving, property 3 of section 2, the updated mixing ratio values ψ and χ at P cannot fall outside the dotted rectangle $R(S_P)$. For a scheme that is both semi-linear in the sense of equations (16) and (43), and "monotone" in the sense of *Harten* [1983], the updated mixing ratio values at P cannot fall outside the boat-shaped polygon A,B,...,E, as shown in Appendix B.

The scheme CD2 is linear (property 1), whereas VL2 and UL4 are nonlinear. In section 7 we examine whether the ability of a numerical model to establish correlations between species is affected by the use of these nonlinear schemes. The question of whether advection schemes preserve preexisting functional relations between different species is addressed in the next two sections.

4. Preservation of Preexisting Functional Relations: Theory

4.1. Linear Functional Relations and Semi-linear Advection Schemes

Advection schemes based on the flux form of the advection equation require the calculation of a mixing ratio χ_f corresponding to each interface between grid boxes. This χ_f is then multiplied by the mass flux of fluid to give the flux of tracer substance between boxes. Generally, χ_f is a function of the grid point values, χ,

$$\chi_f = N(\chi) \tag{14}$$

such that $N(A) = A$ for any constant field A. Concrete examples are given in (44), (49), and (54) below. For flux-limited advection schemes, $N(\chi)$ is nonlinear: for two tracer fields with mixing ratios ψ and χ,

$$N(A\psi + B\chi) \neq A\,N(\psi) + BN(\chi) \tag{15}$$

generally. However, there is a class of flux-limited schemes, including VL2 and UL4, that satisfy

$$N(A\psi + B) = A\,N(\psi) + BN(1) = A\,N(\psi) + B \tag{16}$$

for any constants A and B. Schemes with this property will be called, by definition, "semi-linear." An alternative but equivalent definition is given in (43) below. Being semi-linear in this sense ensures that a scheme will preserve a linear functional relation between two species, even if the scheme is nonlinear. The fact that schemes satisfying (16) preserve linear relations has been noted independently by *Lin and Rood* [1996].

Not all flux-limited schemes are semi-linear in this sense (nor any scheme with negative-value filling). For example, and it is not the only example, *Prather* [1986]

describes an optional limiter for his second-order-moments advection scheme. This limiter prevents the production of negative box-average mixing ratios but does not prevent overshoots, nor undershoots that do not go negative. When such a scheme is applied to two tracer species that are linearly related, say with mixing ratios ψ and $\chi = 1 - \psi$ in the range $(0, 1)$, then one of them could overshoot past 1 whereas the other cannot become negative. Then the linear relation is disrupted. *Lee et al.* [1997] describe disruption of linear relations by this advection scheme and limiter, in simulations of transport and chemistry in the winter stratosphere.

4.2. Nonlinear Functional Relations and "Numerical Mixing"

In Eulerian numerical modeling there is some ambiguity in the idea of preserving a nonlinear functional relation between species. Consider two tracers with mixing ratios ψ and χ, the first with mixing ratio $\psi = 1$ in part of the domain and $\psi = 0$ elsewhere, and the second with mixing ratio $\chi = 0$ where $\psi = 1$, and $\chi = 1$ where $\psi = 0$. When the tracers are advected a distance of half a grid box, some new values of the mixing ratios, other than 0 and 1, are bound to arise. This simple thought experiment illustrates two points. First, there may not be a unique functional relation implied by the initial tracer distribution: for instance, both $\chi = 1 - \psi$ and $\chi = 1 - \psi^2$ hold in this case, and so it is not obvious which, if either, should hold at a later time. Second, and more important, "numerical mixing" is inevitable because of the finite grid resolution [e.g., *Thuburn*, 1995]. This means that no practical Eulerian advection scheme can exactly preserve arbitrary functional relations between species: some spurious scatter is inevitable.

The term "numerical mixing" will be kept in quotes—it might be better to call it "numerical spreading"—because it can be very unlike real mixing. For instance, a linear scheme like CD2 will artificially expand the range of mixing ratios it sees, spreading the values along extrapolated mixing lines, that is, according to formula (13) with λ and μ no longer restricted to lie in the range $(0, 1)$. Such spreading is grossly different from real mixing, because some of the tracer is, on the contrary, being unmixed. This effect can drastically worsen the spurious scatter in a nonlinear functional relation between the mixing ratios of two species, as will be illustrated below in Figure 3c.

A shape-preserving scheme like VL2 or UL4, i.e., a scheme having property **3** of section 2, listed above equation (9), causes "numerical mixing" that is more like real mixing in so far as the scheme never expands the range of mixing ratio values it sees. This result is easily shown as follows. When the scheme is applied for one time step to update the mixing ratio value at a given grid point P, it sees only the mixing ratio values in the grid neighborhood, i.e., only the values at a local set of grid points $\mathsf{S_P}$ consisting of P and some neighboring grid points. It must therefore give the same result at P as if the extreme (maximum and minimum) mixing ratio values for the set $\mathsf{S_P}$ were an absolute maximum and an absolute minimum for the whole domain. Property **3** of section 2 therefore implies that the updated value at P cannot go outside the range spanned by the same maximum and minimum.

Figure 1b illustrates how this result maps into the correlation diagram for two tracers with mixing ratio ψ and χ. The values of (ψ, χ) at the grid points of $\mathsf{S_P}$ map into a finite set of points, $I(\mathsf{S_P})$, say, in the correlation diagram, shown as the filled circles (heavy dots) marked A to E. Regardless of the number of points and their configuration, there is always a smallest axis-oriented rectangle $\mathsf{R(S_P)}$ containing $I(\mathsf{S_P})$. In the case of Figure 1b, $\mathsf{R(S_P)}$ is the dotted rectangle. The shape-preserving property implies that "numerical mixing" cannot, at the grid point P, create a new value that falls outside $\mathsf{R(S_P)}$. The envelope of the set of all such rectangles $\mathsf{R(S_P)}$, for all grid points P, therefore limits the extent to which a shape-preserving scheme can blur or shift a nonlinear functional relation. However, the result still need not resemble the mixing line situation of Figure 1a. Figure 4c below will provide an example in which it clearly does not. In that example the cumulative effect of a shape-preserving scheme, VL2, is mainly a sideways shift to the convex side of a preexisting functional relation. This is very unlike real mixing, which, as suggested in Figure 1a, blurs and shifts a nonlinear functional relation to its concave side only.

If we wish to guarantee that "numerical mixing" resembles real mixing in this last respect, then it seems that we may have to make the scheme satisfy a condition far more restrictive than the shape-preserving property, and to sacrifice accuracy in other respects. The only condition we know of that guarantees "numerical mixing" on the concave side only says that the scheme must be both semi-linear in the sense of equation (16) and "monotone" in the sense of *Harten* [1983]. This last condition is briefly discussed in Appendix B, where the monotone property is defined, and shown to imply both the shape-preserving property and "numerical mixing" to the concave side only. More precisely, the updated mixing ratio values (ψ, χ) at the grid point P cannot fall outside the convex hull of the set $I(\mathsf{S_P})$. This is the smallest convex polygon enclosing all the points of $I(\mathsf{S_P})$; in the example shown in Figure 1b it is the boat-shaped polygon AB...E, much narrower than the rectangle $\mathsf{R(S_P)}$. But Harten shows that monotone schemes are restricted to having only first-order accuracy in grid size—a heavy price to pay. A more accurate scheme, such as VL2 or UL4, cannot be monotone in the required sense.

5. Preservation of Preexisting Functional Relations: Numerical Tests

5.1. Linear Relations

The three schemes described in section 3 and Appendix A were tested in some simple one-dimensional experi-

ments. Four initial tracer profiles, $\psi_i (i = 1, \ldots, 4)$, were set up (Figure 2a) and advected by a constant wind once around a periodic domain of 48 regularly spaced grid points at a Courant number $c = 0.2$, equation (46) below. Then four more tracer profiles χ_i $(i = 1, \ldots, 4)$ were set up. These are linearly related to the first four according to $\chi_i = -0.8\psi_i + 0.9$. The second set of tracers were also advected once around the periodic domain.

As expected, CD2 produces spurious oscillations and negative mixing ratios in the tracer fields, and three of the four tracer profiles are badly distorted (Figure 3a). VL2 produces no spurious oscillations, though there is some flattening of extrema and a tendency to steepen some gradients (Figure 4a,b). (This nonlinear, antidiffusive steepening is explained in Appendix A2, and warns us not to take terminology like "shape preserving" too literally.) UL4 is arguably better than VL2, with a much slighter flattening of extrema in the top right and bottom left panels of Figure 5a, for instance, albeit some small-scale distortions (of the kind sometimes called "staircasing"), especially noticeable in the bottom right panel of Figure 5a and the top right of 5b. These will be relevant in section 7.1. As predicted in section 4.1, all three schemes exactly preserve the linear relations between the sets of tracers (plots not shown).

5.2. Nonlinear Relations

Another set of tests was carried out in which the second set of tracers was nonlinearly related to the first according to $\chi_i = -0.8\psi_i^4 + 0.9$. The initial distributions of the second set of tracers and their correlation diagrams with the first set are shown in Figures 2b and 2c. The results of advecting the tracers using the three schemes, and the final correlation diagrams, are shown in Figures 3, 4, and 5. Again the final tracer profiles show that VL2 and UL4 are far superior to CD2 in maintaining tracer profiles with sharp changes of gradient, UL4 being distinctly better than VL2.

The correlations for the square wave profile illustrate the ambiguity discussed in section 4.2. Initially, there are only two points on the correlation diagram, the top left panel of Figure 2c, and these do not define any particular functional relation. All three schemes generate new tracer values that are linearly related, as shown in the top left panels of Figures 3c, 4c and 5c.

The linear scheme CD2 distorts and scatters two of the remaining three functional relations (Figure 3c), confirming that, as expected, linearity of an advection scheme is not enough to ensure the preservation of arbitrary functional relations. VL2 is better, and UL4 is better still with relatively slight scatter.

In the tests discussed so far, no attempt has been made to fill in the negative mixing ratios produced by CD2. Such filling is often used in numerical models. Figure 6 clearly shows how such filling turns CD2 into a nonlinear scheme, CD2F say, which disrupts the linear functional relations in the first set of test cases, most of all in the case of the step profile. *Allen et al.* [1991] give an example of disruption of functional relations by negative-value filling in a three-dimensional chemical transport model, and avoidance of that disruption

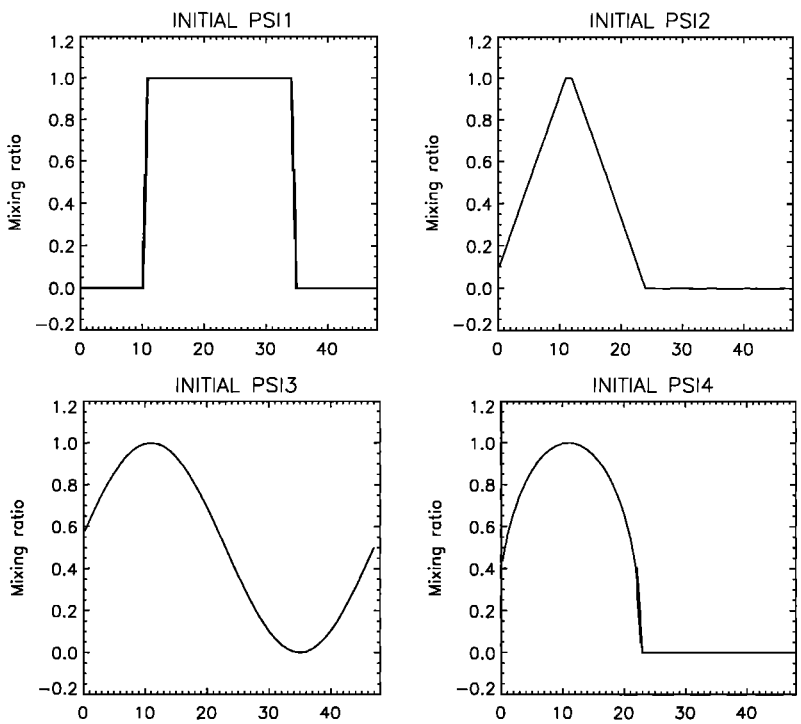

Figure 2a. Initial conditions for the one-dimensional spatial distributions of the first set of tracers, ψ_i $(i = 1, \ldots, 4)$, in the experiments to test preservation of linear and nonlinear functional relations.

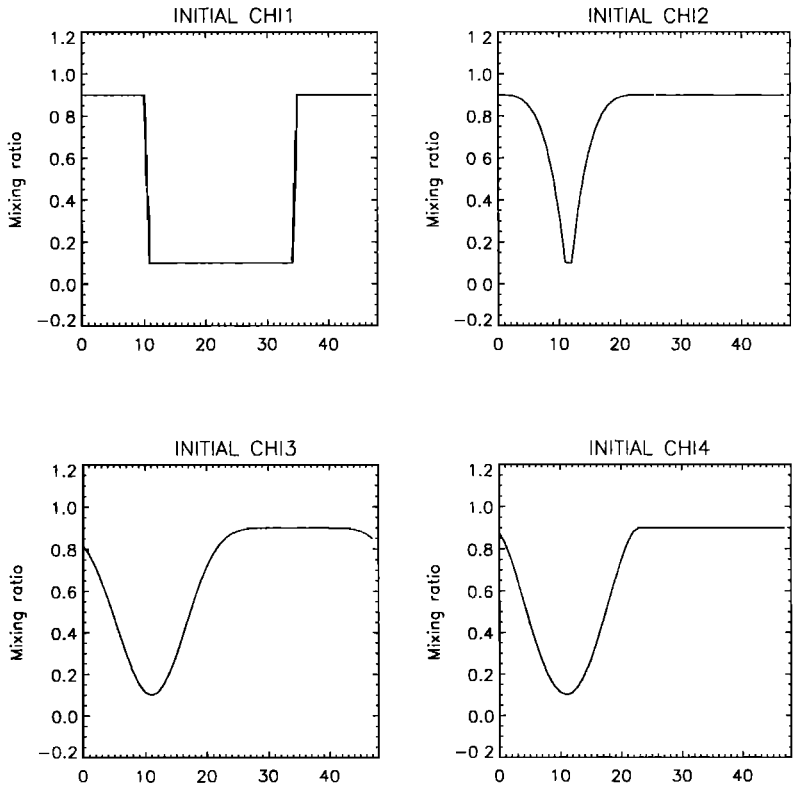

Figure 2b. Initial conditions for the one-dimensional spatial distributions of the second set of tracers, χ_i $(i = 1, \ldots, 4)$, in the experiment to test preservation of nonlinear functional relations. These are related to the first set by $\chi_i = -0.8\psi_i^4 + 0.9$.

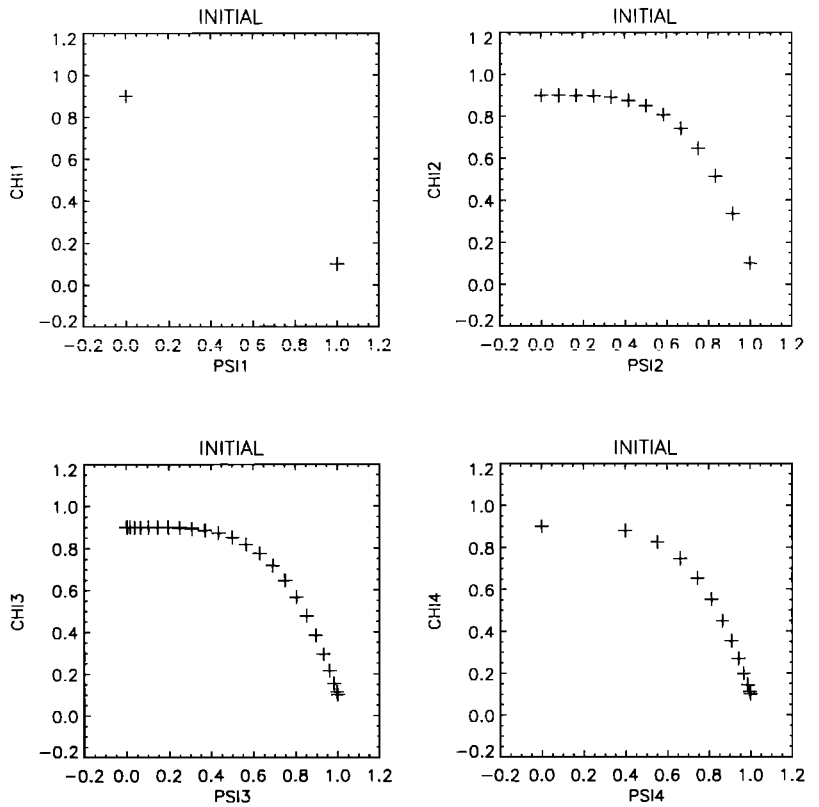

Figure 2c. Correlation diagrams showing the initial correlations, consistent with the nonlinear functional relation $\chi_i = -0.8\psi_i^4 + 0.9$, between the two sets of tracers in the experiment to test preservation of nonlinear functional relations. Here ψ_i is plotted along the horizontal axis, and χ_i is plotted along the vertical axis.

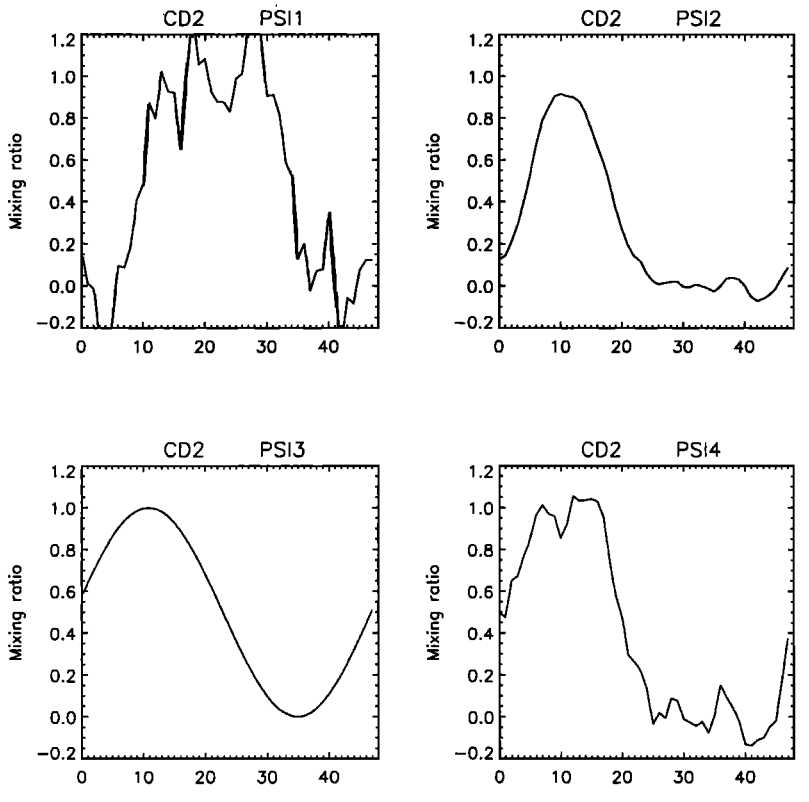

Figure 3a. Final distributions of the first set of tracers, ψ_i, in the experiments to test preservation of linear and nonlinear relations using scheme CD2.

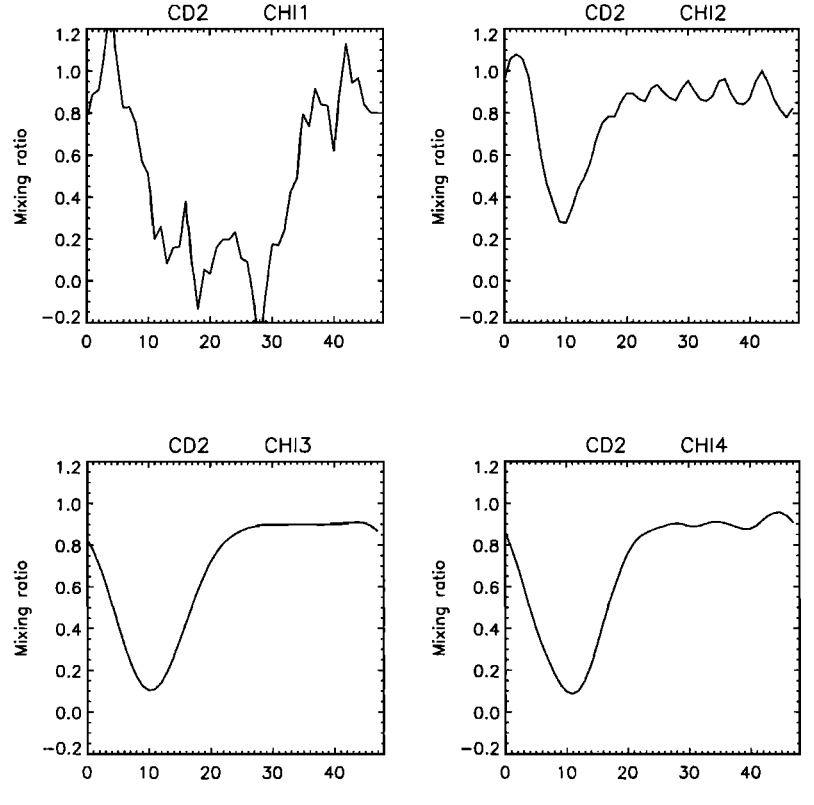

Figure 3b. Final distributions of the second set of tracers, χ_i, in the experiment to test preservation of nonlinear relations using scheme CD2.

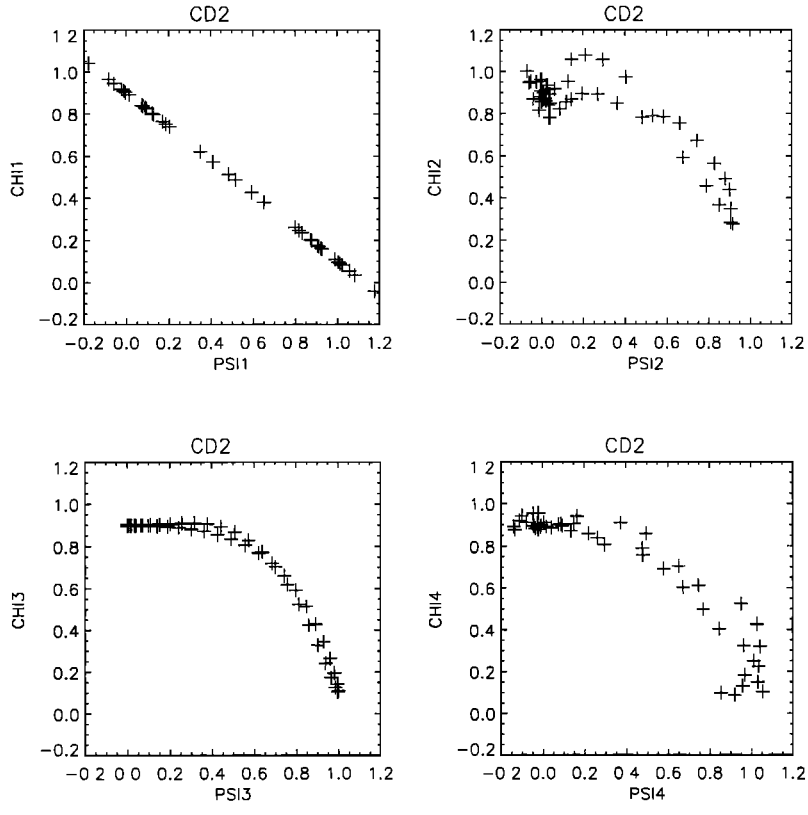

Figure 3c. Correlation diagrams showing final correlations between ψ_i and χ_i in the experiment to test preservation of nonlinear relations using scheme CD2.

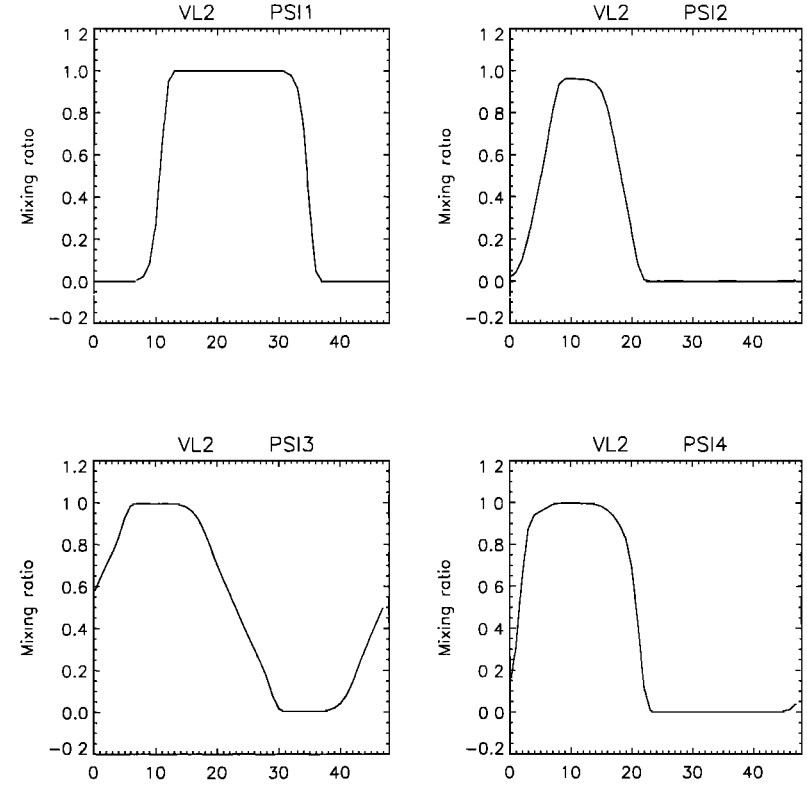

Figure 4a. Final distributions of the first set of tracers, ψ_i, in the experiments to test preservation of linear and nonlinear relations using scheme VL2.

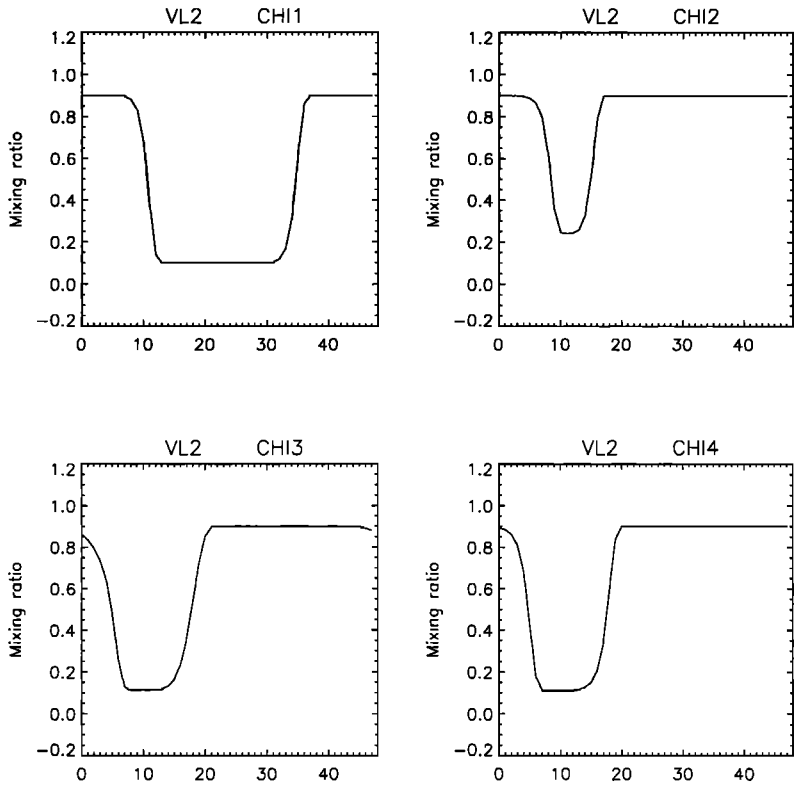

Figure 4b. Final distributions of the second set of tracers, χ_i, in the experiment to test preservation of nonlinear relations using scheme VL2.

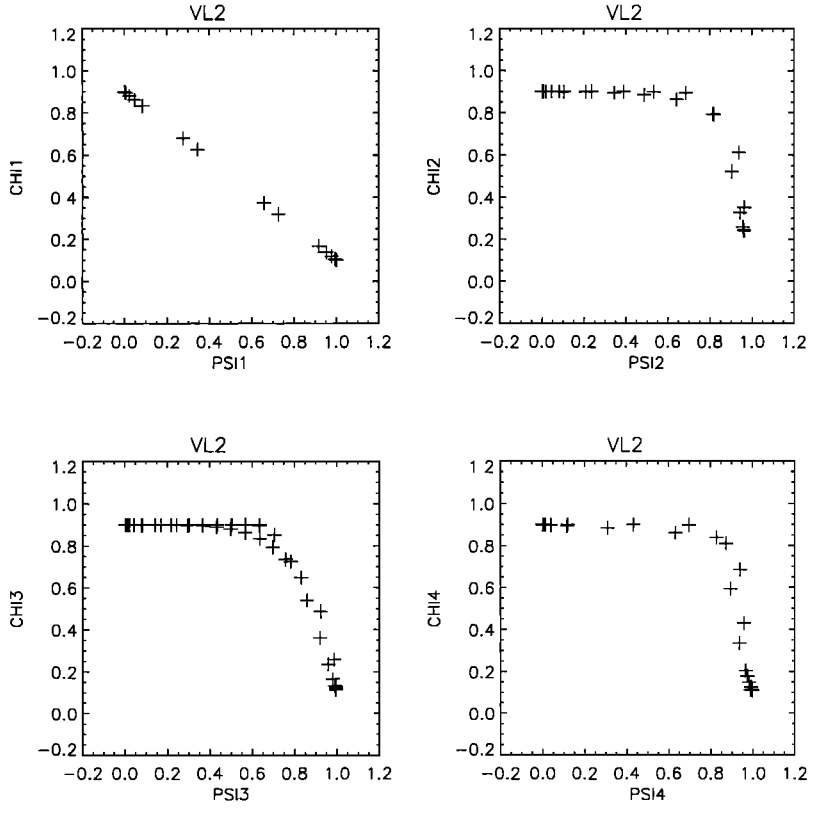

Figure 4c. Correlation diagrams showing final correlations between ψ_i and χ_i in the experiment to test preservation of nonlinear relations using scheme VL2.

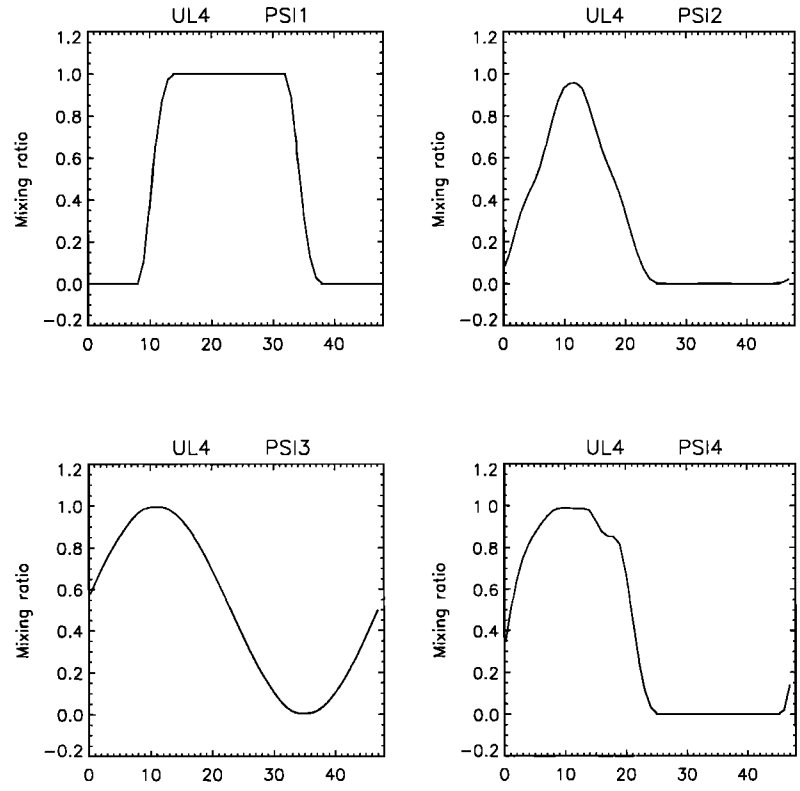

Figure 5a. Final distributions of the first set of tracers, ψ_i, in the experiments to test preservation of linear and nonlinear relations using scheme UL4.

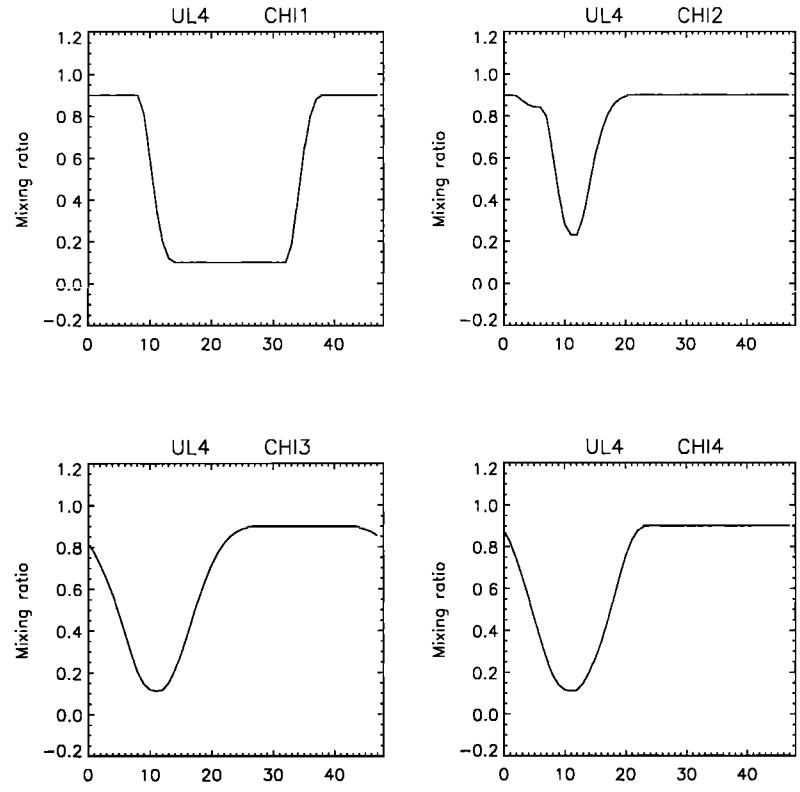

Figure 5b. Final distributions of the second set of tracers, χ_i, in the experiment to test preservation of nonlinear relations using scheme UL4.

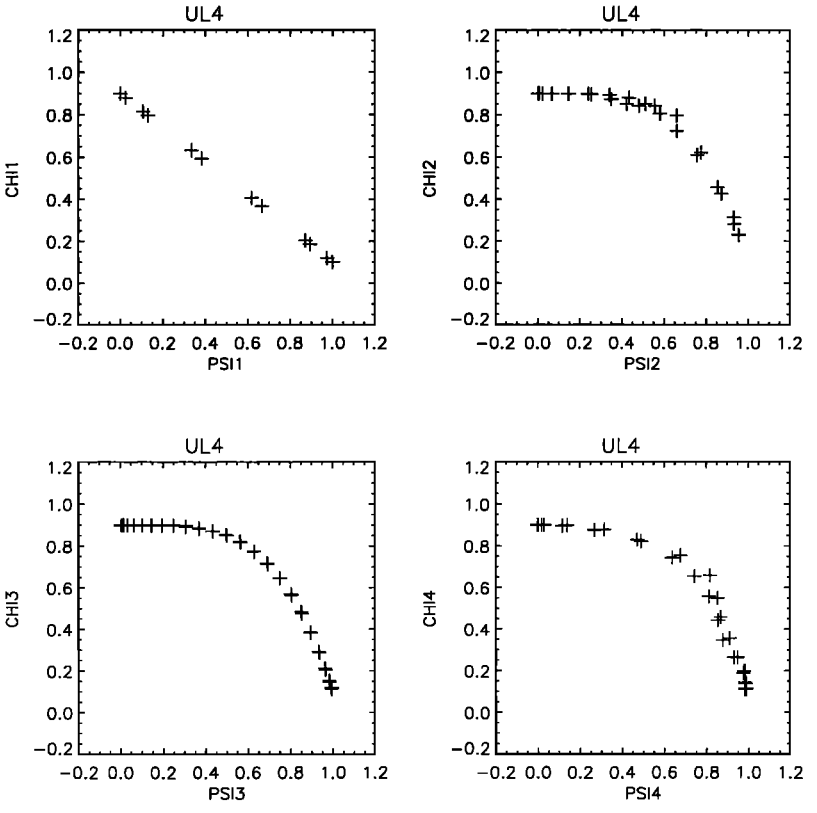

Figure 5c. Correlation diagrams showing final correlations between ψ_i and χ_i in the experiment to test preservation of nonlinear relations using scheme UL4.

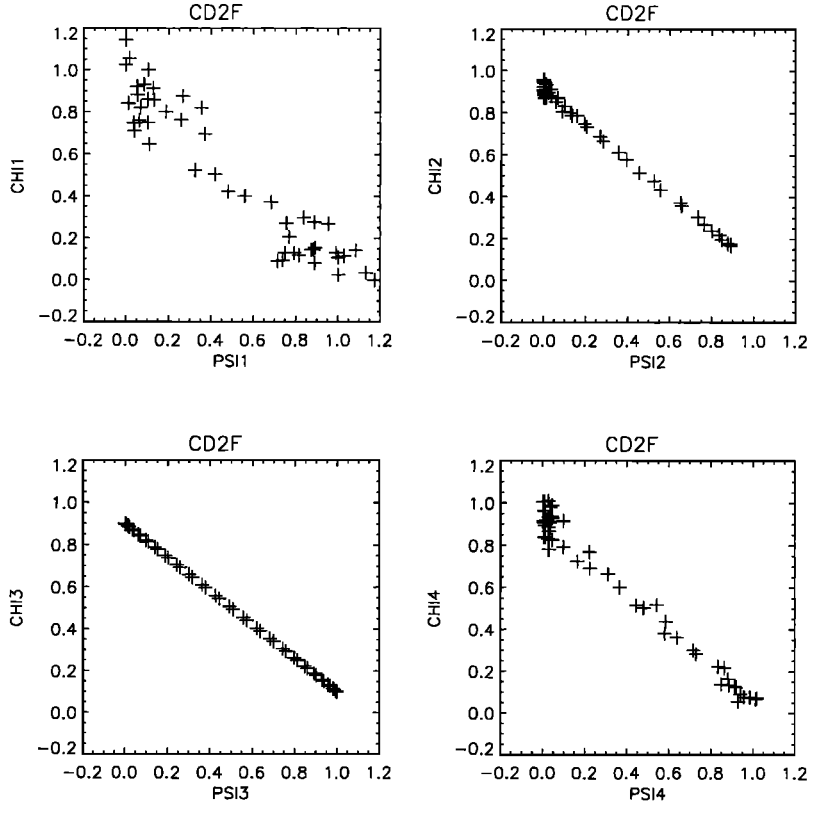

Figure 6. Correlation diagrams showing final correlations between the sets of tracers in the experiment to test preservation of linear relations using scheme CD2 with filling of negatives. Here ψ_i is plotted along the horizontal axis, and χ_i is plotted along the vertical axis.

by changing to a flux-limited advection scheme. The nonlinear relations in the second set of test cases that are already strongly disrupted by CD2 without filling (Figure 3c, top right and lower right) suffer little additional effect from filling (not shown).

6. Correlations Established by Transport

PM and PK, and more recently *Plumb* [1996], have pointed out some of the circumstances in which correlations or functional relations are established by transport. The question of how numerical schemes would behave in such circumstances is addressed in section 7 after reviewing and extending the results of PM and PK in this section. Our main motivation here is to expose as clearly as possible the assumptions used in the derivation, so that their compatibility with properties of numerical transport algorithms can be looked at in section 7. The analysis also leads to the aforementioned generalization, equation (40) below, of the result on stratospheric vertical diffusion given in PK and its predecessors. Some of the results hold only in an ensemble-mean sense, implying correlations with scatter rather than perfect functional relations.

The starting point is equation (3) generalized to include chemical sources and sinks, i.e.,

$$\frac{\partial \chi}{\partial t} + L(\chi) = S(\chi) - \Lambda(\chi) \tag{17}$$

where $S(\chi)$ represents sources for χ and $\Lambda(\chi)$ represents sinks for χ and, where, as before, $L(.)$ is a linear operator representing gas-phase transport. As already noted, linear transport preserves linear functional relations $\chi = A\psi + B$ in the absence of chemical sources and sinks. It can be seen from (17) and its counterpart for ψ that such functional relations are also preserved in the presence of sources and sinks, provided that the source–sink distributions for ψ and χ are proportional with proportionality constant A, i.e., provided that

$$S(\chi) - \Lambda(\chi) = A(S(\psi) - \Lambda(\psi)) \tag{18}$$

For, substituting (18) into the right of (17), we immediately find that the resulting equation is satisfied by $\chi = A\psi + B$ if we use the linearity property of $L(.)$. Assuming that (17) with initial and boundary conditions is a well-posed, as well as a linear, problem, we may deduce that if $\chi = A\psi + B$ initially and at the domain boundaries then $\chi = A\psi + B$ everywhere and for all subsequent times t. This makes precise, in great generality, the idea mentioned below equation (1) in the Introduction that, for two gas-phase species with "common sources and sinks," the transport, under suitable assumptions, shapes their mixing ratio fields ψ and χ "in the same way." It is sometimes useful to interpret (18) and its consequences in an ensemble-mean sense.

PM analyzed an interesting subclass of this general class of situations, in which certain assumptions about timescales hold, simplifying the role of $\partial/\partial t(.)$ and replacing the general stipulation of well-posedness by an assumption that $L(.)$, with suitable boundary conditions understood, is invertible up to an additive constant. They used the term "gradient equilibrium" to denote such situations. The word "gradient" refers to the property that $L(B) = 0$ when B is a constant, which implies that $L(.)$ sees only gradients (and higher derivatives) of its argument; that is, $L(.)$ is indifferent to additive constants and sees only the way in which a tracer mixing ratio field varies in space. The word "equilibrium" refers to the assumptions about timescales, which are consistent with assuming that that the system has forgotten the initial conditions and that it is either steady or close to steadiness. PM's assumptions appear relevant to understanding the behavior of long-lived tracers in the troposphere (PM) and in the stratosphere (PK), and the way in which correlations between them can be established by transport, regardless of initial conditions.

6.1. PM's Example of Gradient Equilibrium

Following PM, we assume that the transport represented by $L(\chi)$ in equation (17) involves mixing and tends to homogenize χ throughout the domain of interest, D say. Consistently with this (cf. remark below (27)), we assume that the operator $L(.)$ is invertible up to an additive constant. Again following PM, we treat S as prescribed and Λ as a function of the local value of χ whose sense is relaxational. By relaxational we mean that $\Lambda(\chi)$ is a monotonically increasing function of χ. The homogenization is assumed to be relatively fast in the sense that its longest timescale τ_T is much shorter than the other relevant timescales. These latter are the shortest chemical timescale τ_C and the shortest timescale τ_U for unsteadiness in the tracer distribution, governing the magnitude of $\partial\chi/\partial t$ in (17). In summary,

$$\tau_T \ll \tau_C, \tau_U \tag{19}$$

We introduce a small parameter $\varepsilon = \tau_T / \min(\tau_C, \tau_U)$ and a slow time variable

$$\tau = t/\min(\tau_C, \tau_U) = \varepsilon t/\tau_T \tag{20}$$

and assume that χ, S, and Λ are functions of position $\mathbf{x}$ and slow time τ alone, with $\partial/\partial\tau \lesssim 1$. Consistently with these scaling assumptions, we expand χ in powers of ε,

$$\chi = \chi_0(\mathbf{x}, \tau) + \varepsilon\chi_1(\mathbf{x}, \tau) + \ldots \tag{21}$$

and make appropriate rescalings of S and Λ:

$$S = \varepsilon S_1(\mathbf{x}, \tau)/\tau_T \tag{22}$$

$$\Lambda = \varepsilon\Lambda_1(\chi(\mathbf{x}, \tau))/\tau_T \tag{23}$$

The domain D may be the whole atmosphere. Alternatively, we may restrict attention to some subdomain provided that the transport of tracer through the boundary of the subdomain is not strong enough to vi-

olate the scaling assumptions, for instance by producing strong inhomogeneity or large unsteadiness near the boundary. Assuming no such violation, we note that then

$$\langle L(\chi)\rangle = -\varepsilon C_1(\tau)/\tau_T + O(\varepsilon^2) \tag{24}$$

where the angle brackets denote a mass-weighted average over the domain D, and where C_1 scales like S_1 and Λ_1 and is finite as $\varepsilon \to 0$. We shall further assume that to leading order in ε there is no net influx through the boundary; that is, $C_1 = 0$.

Now use the assumption that $L(.)$ is linear. Then, with (21),

$$L(\chi) = L(\chi_0) + \varepsilon L(\chi_1) + \ldots \tag{25}$$

Substituting (25) into (17) and using (22)–(23) to neglect the right hand side, we obtain at leading order in ε

$$L(\chi_0) = 0 \tag{26}$$

Because of the homogenization and invertibility assumptions, equation (26) implies that the gradients of χ_0 vanish, i.e., that χ_0 is a function of the slow time τ alone and not of position $\mathbf{x}$:

$$\chi_0 = \chi_0(\tau) \tag{27}$$

The homogenization and invertibility assumptions are essential here: for instance the gradients of χ_0 would not need to vanish if $L(.)$ represented purely advective transport parallel to the isopleths of a steady tracer field, with no mixing involved. Note incidentally that homogenization and invertibility are not logically equivalent (as can be shown by counterexample) though they often go together. This is discussed in section 7.1.

At order ε, (17) gives

$$\frac{\partial \chi_0}{\partial \tau} + L(\chi_1) = S_1 - \Lambda_1(\chi_0) \tag{28}$$

Averaging this over the domain D and using (24) with $C_1 = 0$ gives

$$\frac{\partial \chi_0}{\partial \tau} = \langle S_1\rangle - \langle \Lambda_1(\chi_0)\rangle \tag{29}$$

which, combined with (28), gives, as PM found,

$$L(\chi_1) = \big(S_1 - \langle S_1\rangle\big) - \big(\Lambda_1(\chi_0) - \langle \Lambda_1(\chi_0)\rangle\big) \tag{30}$$

If we further assume either that the sink is uniform over the domain ($\Lambda_1 \approx \langle \Lambda_1\rangle$) or that the sinks are much weaker than the average source, $\Lambda_1(\chi_0) \ll \langle S_1\rangle$, then (30) becomes simply

$$L(\chi_1) \approx S_1 - \langle S_1\rangle \tag{31}$$

In this case we see, again using the invertibility assumption, that gradients of χ_1 and therefore of χ depend only on $S_1 - \langle S_1\rangle$, and that they do so linearly though nonlocally. In symbols, $\chi_1 \approx L^{-1}(S_1 - \langle S_1\rangle)$.

PM's results (30) and (31), taken together with the invertibility assumption, are important special cases of the more general result noted earlier, below (18), on the "shaping" of tracer fields by transport such that linear functional relations are preserved. Two tracer fields whose spatially variable parts $\chi_1^{(1)}$ and $\chi_1^{(2)}$ both satisfy (31), for instance, with $S_1 = S_1^{(1)}$ and $S_1 = S_1^{(2)}$, respectively, will be linearly related if and only if the ratio $(S_1^{(1)} - \langle S_1^{(1)}\rangle)/(S_1^{(2)} - \langle S_1^{(2)}\rangle)$ is approximately constant in space and time; cf. (18).

6.2. Generalized Slope Equilibrium

Consider a domain D within the stratosphere with the vertical direction labeled by a coordinate z, equal to some function of potential temperature θ, and the horizontal direction labeled by coordinates $\mathbf{x}$; D might for instance represent a stratospheric surf zone. It will be convenient to choose $z = H_\theta \log(\theta/\theta_0)$, where H_θ is a scale height for potential temperature (about 25 km) and θ_0 is a constant, so that z is not very different from the geometric height. Let the timescales for horizontal and vertical transport be τ_H and τ_V respectively, and assume in place of (19)

$$\tau_H \ll \tau_V \lesssim \tau_C, \tau_U \tag{32}$$

with τ_C the timescale for chemistry and τ_U the timescale for unsteadiness of the tracer field, as before. In contrast with the analysis of section 6.1, we now make the homogenization assumption for horizontal transport only, so that τ_H, not τ_V, has the role of the previous fast timescale τ_T. This is expected to be reasonable for long-lived species in the stratosphere, where the horizontal surfaces may be identified, to a first approximation, with the isentropes z = constant and where cross-isentropic transport is far weaker than in the troposphere. Finally, as in section 6.1, we need to assume that transport into or out of the domain D at its periphery is weak enough not to change the picture.

The results now to be derived generalize those of Mahlman, Holton, and PK in three ways. First, we avoid the assumption that horizontal mixing is global in extent. (We note that the independent work of *Plumb* [1996] also avoids this assumption.) Second, we avoid describing the horizontal mixing in terms of a Fickian eddy diffusivity, because it may well not be Fickian in real stratospheric surf zones, as mentioned earlier. Third, to emphasize certain generalities we relax, in part of what follows, the assumption of fast horizontal mixing and homogenization, replacing it by an assumption of fast horizontal particle dispersion, with or without mixing. The picture then holds in the ensemble-mean sense, though not necessarily for each realization.

In all the cases to be discussed—involving fast horizontal transport in one sense or other, on the fast timescale τ_H—we shall have, to a first approximation, at least in the ensemble-mean sense,

$$\chi \approx \chi(z,t) \tag{33}$$

Therefore, at least in the ensemble-mean sense, any two species whose mixing-ratio fields are thus shaped will be functionally related, at any particular time, not for the reasons discussed below (18) but simply because each mixing ratio, or the ensemble mean of each, is a function of z alone. This brings in an entirely new possibility, namely, that nonlinear functional relations can arise. PK used the term "slope equilibrium" to denote such situations. Here the word "slope" refers to the fact that the mixing-ratio isopleths will generally have finite slopes. Following (and also generalizing) PK, we will show that

$$\chi \approx \chi(Z,t) \tag{34}$$

to better approximation than (33), where Z is another vertical coordinate whose isosurfaces slope slightly with respect to z surfaces, possibly in a longitude and time varying way.

Consider the motion of a material particle in this class of situations. It will move quickly from place to place on, or almost on, a z surface. Its weaker motions in the z or cross-isentropic direction will depend on where it lies on the z surface, specifically, on whether it finds itself in a region of diabatic ascent or descent. Such regions may themselves be moving horizontally, and changing size and shape, for instance because of the baroclinic dynamics of synoptic-scale or surf zone eddies. If the net effect is equivalent to small random fluctuations in the particle's diabatic heating rate, then the z motion will have the character of a random walk with small vertical steps, added to any Lagrangian-mean vertical drift.

In an ensemble mean, with the horizontal cross-sectional area of the domain D randomly sampled by particles, the effect of such a random walk is approximately equivalent, as is well known, to one-dimensional Fickian vertical diffusion together with a one-dimensional Lagrangian-mean vertical drift. The latter, being one-dimensional, a function of z only, is equivalent to an Eulerian-mean vertical mass flux $\overline{\rho w}$, giving approximately

$$\overline{F(\chi)} = \overline{\rho w}\,\overline{\chi} - \bar{\rho} K \overline{\chi}_z \tag{35}$$

Here the overbar denotes the ensemble and horizontal area mean, $F(\chi)$ is the flux of tracer substance across the z surface, $w = Dz/Dt$, the diabatic vertical velocity, suffix z denotes the vertical derivative, K is the effective vertical diffusion coefficient in the z direction, describing the mean effect of the vertical random walk, and ρ is now defined in such a way that the mass element $dm = \rho dx dy dz$ in these coordinates.

The one-dimensional version of a well-known argument [*Taylor*, 1921] shows that the value of K is given by $\int_0^\infty \overline{w''(t)w''(t-\tau)}^{\mathrm{LE}} d\tau$, where the overbar with superscript "LE" denotes a suitably weighted Lagrangian ensemble mean, double primes denote the randomly fluctuating contributions, and the arguments t and $t-\tau$ refer to the same particle at different times. The integrand is the relevant Lagrangian velocity autocovariance, in which the double prime denotes a Lagrangian fluctuation, not an Eulerian one. So the most general conditions for getting the behavior (35) are those under which (a) the Lagrangian velocity autocovariance is statistically stable, and such that the above integral is well defined (integrand evanescent, not strongly oscillatory), and (b) there is sufficient uniformity in time and in the horizontal, and sufficient uniformity in vertical gradients, on timescales $\gg \tau_H$, for Taylor's argument to apply: in particular, the Eulerian-mean gradient $\overline{\chi}_z$ can be taken also as an approximately uniform background gradient when doing Lagrangian averaging.

The conditions under which (35) holds include two opposite extreme cases: first, that of a steady, geographically fixed diabatic heating pattern $w(\mathbf{x})$ and random horizontal particle motion, and second, that of steady horizontal particle motion and randomly changing diabatic heating pattern $w(\mathbf{x},t)$. Although the first extreme is usually assumed, for instance in the papers by PK and by *Holton* [1986] and *Mahlman et al.* [1986], the real situation is presumably somewhere between the two extremes. Recent estimates of particle trajectory statistics in stratospheric surf zones from observational data (L. C. Sparling et al., Diabatic cross-isentropic dispersion in the lower stratosphere, submitted to *Journal of Geophysical Research*, 1997) suggest that the real situation is closer to the first extreme. The same estimates—which include direct estimates of surf-zone Lagrangian velocity autocovariances and evidence for their statistical stability—show ensemble-mean behavior consistent with (35), with $K \sim 0.2\ \mathrm{m^2 s^{-1}}$.

Note that this K is not a simple turbulent eddy diffusivity, in the classical sense of weakly inhomogeneous turbulence theory. Such theories are hardly ever applicable, because of the extreme spatial inhomogeneity of real, naturally occurring turbulence. Rather, K is a "shear-dispersive diffusivity" depending jointly on the fast horizontal transport and on the steady or unsteady differential vertical advection [*Taylor*, 1953; *Holton*, 1986; *Mahlman et al.*, 1986; PK]. As the foregoing argument makes clear, and as equation (40) will confirm, the well-definedness of K does not depend on any scale separation in the horizontal. In particular, it does not depend on whether the horizontal transport can be described as Fickian diffusion. If we think of the horizontal transport as particle dispersion by a random walk, then there is no requirement for the horizontal steps to be small in any sense, as indeed they might well not be in a real stratospheric surf zone.

In addition to the K in (35), there may be a vertical diffusivity due to intermittent mixing in small-scale, three-dimensional turbulent layers, producing an additional vertical random walk [*Dewan*, 1981]. The resulting vertical diffusivity will combine additively with the K of equation (35) if the two random walks are statistically independent.

Equation (35) can also be derived within the Eulerian framework, again avoiding assumptions of scale separation or Fickian eddy diffusion in the horizontal. To do this, we represent the fast horizontal transport by a linear operator $H(\chi')$ analogous to the $L(\chi)$ of (3) and (17), with single primes denoting a departure from the horizontal area mean. Thus single primes denote an Eulerian, not a Lagrangian, fluctuation. We use suffixes to denote derivatives and replace (17) by

$$\chi'_t + H(\chi') + \overline{w}\chi'_z + w'\overline{\chi}_z + w'\chi'_z = S' - \Lambda' \qquad (36)$$

where $H(.)$ is taken to satisfy the homogenization and invertibility assumptions, either for individual realizations or in the ensemble-mean sense. Note that, with $\overline{\chi'} = 0$ by definition, there is no undetermined additive constant: invertibility now says that the field χ' is uniquely obtainable from the field $H(\chi')$. Note that the linearity property implies $\overline{H(\chi')} = 0$. Also, $H(.)$ is taken to be indifferent to vertical gradients, seeing only the horizontal structure of the χ' field at constant z.

Recalling the scaling assumptions (32), we see that the dominant balance in (36) will be between the second and fourth terms, under reasonable further assumptions. Let X be a typical vertical variation in $\overline{\chi}$, let ηX be a typical value of χ' (η to be determined), and let W be a typical value of w', assumed $\gtrsim \overline{w}$ and $\gtrsim \overline{\rho w}/\bar{\rho}$, so that $\tau_V W$ is a corresponding height scale, which latter we identify with $X/\overline{\chi}_z$, assumed $\lesssim \eta X/\chi'_z$. The terms in (36) scale respectively as $\chi'_t \sim \eta X/\tau_U$, $H(\chi') \sim \eta X/\tau_H$, $\overline{w}\chi'_z \lesssim w'\chi'_z \sim \eta X/\tau_V$, $w'\overline{\chi}_z \sim X/\tau_V$, $S' - \Lambda' \sim \eta X/\tau_C$. Under the assumed conditions, there is no term that can balance $H(\chi')$ except $w'\overline{\chi}_z$. So there can be a balance in (36) if and only if

$$\eta \sim \tau_H/\tau_V \ll 1$$

implying that χ' is small in comparison with vertical variations in $\overline{\chi}$. Then (36) reduces to $H(\chi') + w'\overline{\chi}_z = 0$, with relative error $O(\eta)$, from which it follows, with the same relative error, that

$$\chi' = -\overline{\chi}_z H^{-1}(w') \qquad (37)$$

where the linearity property, the invertibility assumption, and the indifference of $H(.)$ to vertical gradients have all been used; $H^{-1}(.)$ denotes the inverse of $H(.)$ and is a linear operator.

The vertical flux of tracer substance per unit area across a z surface is (again neglecting small-scale turbulent mixing)

$$F(\chi) = \rho w \chi \qquad (38)$$

so that the corresponding mean flux is

$$\overline{F(\chi)} = \overline{\rho w}\ \overline{\chi} + \overline{(\rho w)'\chi'} \qquad (39)$$

But, because of (37), $\overline{(\rho w)'\chi'} = -\overline{\chi}_z\, \overline{(\rho w)' H^{-1}(w')}$, showing that, with relative error $O(\eta)$, (39) is equivalent to (35) with the vertical diffusivity

$$K = \bar{\rho}^{-1}\, \overline{(\rho w)' H^{-1}(w')} \qquad (40)$$

Note that the inverse horizontal transport operator $H^{-1}(.)$ has dimensions of time, and order of magnitude τ_H giving $K \sim \tau_H W^2$. Thus if we make the horizontal transport faster, for instance, so that τ_H is smaller, then we get a smaller value of K. This is exactly as expected from the Lagrangian picture, because the vertical (diabatic) random walk must then have smaller steps, for any given w' field. It is also consistent with the classic results on shear-dispersive diffusivity [e.g., *Taylor*, 1953] and with the results obtained by *Holton* [1986], *Mahlman et al.* [1986], and PK, which assumed simplified, steady horizontal diabatic heating patterns of the form $w(\mathbf{x}, t) = w(y)$, where y is latitude, together with horizontal Fickian diffusion of the form $H(\chi') = H(\chi'(y)) = -(K_{\text{horiz}}\chi'(y)_y)_y$.

The field $H^{-1}(w')$ has dimensions of length and order of magnitude $\ll \tau_V W$, the height scale of the mean tracer field: $H^{-1}(w') \sim \tau_H W \sim \eta\tau_V W \ll \tau_V W$. We note that $H^{-1}(w')$ has two physical interpretations. First and most simply, it describes the vertical displacement of tracer isopleths relative to isentropes. If we define a new vertical coordinate $Z(\mathbf{x}, z, t)$ by

$$z = Z + H^{-1}(w') \qquad (41)$$

then, recalling (37), we see that, to the first order in $H^{-1}(w')$ considered as a small quantity, $\chi(\mathbf{x}, z, t) = \overline{\chi}(z) + \chi'(\mathbf{x}, z, t) \approx \overline{\chi}(Z + H^{-1}(w')) - \overline{\chi}_z H^{-1}(w') \approx \overline{\chi}(Z)$, which is constant when Z is constant. That is, the surfaces $Z =$ constant coincide with the isopleths of χ, to the first order in small vertical displacements, i.e., more accurately than in the first approximation $z =$ constant. This justifies (34). Moreover, $H^{-1}(w')$ is independent of χ, and so the slopes, more generally the time-dependent undular shapes, of the tracer isopleths are the same for any other tracer satisfying the scaling assumptions. This is PK's "slope equilibrium" regime, now generalized to include the possibility of arbitrary tracer isopleth shapes—time-dependent and longitude-dependent as well as latitude-dependent.

The second physical interpretation of $H^{-1}(w')$ applies whenever we can think of the horizontal transport as a fast random walk (with arbitrary horizontal step size). Then $H^{-1}(w')$ is a measure of the vertical step size of the accompanying cross-isentropic random walk. This interpretation follows from the scaling assumptions (32), which imply that, to a first approximation, a material particle conserves its tracer mixing ratio, i.e., stays on a single tracer isopleth, during its horizontal excursions across substantial parts of the domain D. But this means that random vertical particle displacements, relative to isentropes, must be of the same order as ensemble-mean tracer isopleth displacements relative to isentropes. These in turn, by (41)ff. applied to the ensemble-mean picture, are given by $H^{-1}(w')$. The scaling relation $H^{-1}(w') \ll \tau_V W$ confirms once again that, regardless of the horizontal step size, the vertical step size is small in the sense required to get the Fickian behavior expressed by (35).

Because the results derived so far in this section can be interpreted as ensemble means, they depend only on having fast horizontal particle dispersion, and not on the homogenization assumption in its full sense connoting fast horizontal mixing. Let us now, however, revert to the homogenization assumption in its full sense, with the implication that generalized slope equilibrium will now apply to instantaneous tracer mixing-ratio values, leading to linear or nonlinear functional relations between those values and not just their ensemble means. The observed functional relations, with small scatter, support this assumption as realistic. Consider any two tracer fields in generalized slope equilibrium, with mixing ratios χ and ψ. Their vertical fluxes take the form (35)—or, for improved accuracy, (35) with z replaced by Z—with the same $\overline{\rho w}$ and K for both tracers. So the implied functional relation $\chi = \chi(\psi)$ must satisfy

$$\frac{d\chi}{d\psi} = \frac{\chi_Z}{\psi_Z} = \frac{\overline{F(\chi)} - \overline{\rho w}\,\chi}{\overline{F(\psi)} - \overline{\rho w}\,\psi} \tag{42}$$

If $\overline{\rho w} \approx 0$, as for instance when the domain D has global extent then, as pointed out by PK, $d\chi/d\psi$ is given by the flux ratio $\overline{F(\chi)}/\overline{F(\psi)}$, at each Z. Then the functional relation is linear ($d\chi/d\psi$ = constant) if the fluxes are Z-independent, as may happen if conditions are nearly steady and chemical sources and sinks locally negligible, i.e., if we replace (32) by a three-way timescale separation $\tau_H \ll \tau_V \ll \tau_C, \tau_U$.

If we relax the assumption $\overline{\rho w} \approx 0$, but retain the three-way timescale separation so that the fluxes $\overline{F(\chi)}$ and $\overline{F(\psi)}$ are still Z-independent, then there is still one case in which the functional relation $\chi = \chi(\psi)$ always remains linear, namely when $\overline{\rho w}$ is nonzero but Z-independent. This happens if, for instance, there is negligible mass flux through the sides of the domain D, as with a non-leaky "tropical pipe" model of the stratosphere [*Plumb*, 1996]. Note incidentally that the scaling assumptions allow $\overline{\rho w} \sim \eta\,\bar{\rho} w' \ll \bar{\rho} w'$, the condition for both terms on the right of (35) to be equally significant. Under these conditions, (42), regarded as an ordinary differential equation for $\chi = \chi(\psi)$, has as its most general solution $\overline{F(\chi)} - \overline{\rho w}\,\chi = A\,(\overline{F(\psi)} - \overline{\rho w}\,\psi)$ where A is an arbitrary constant. Because all quantities except χ and ψ are constant, this general solution has the linear form $\chi(\psi) = A\psi + B$.

By considering possible sources, sinks and unsteadiness within and outside the domain D, we can view all these cases of linear functional relations as cases of gradient equilibrium in a larger domain containing D, consistently with (18)ff. Conversely, $\chi(\psi)$ can be nonlinear in some cases where transport through the sides of the domain is significant, as with leaky tropical pipes [e.g., *Boering et al.*, 1996; *Minschwaner et al.*, 1996; *Mote et al.*, 1996; *Plumb*, 1996; *Volk et al.*, 1996], and when unsteadiness or chemical sources or sinks are significant [PK], within or outside the domain D.

7. Correlations Preserved or Established by Numerical Transport

This section discusses to what extent the transport regimes just analyzed can be simulated by numerical models, even though the transport operators $L(.)$ of such models cannot, in practice, be linear. We consider numerical transport operators L that are semi-linear in the sense defined by (16), implying that

$$L(A\chi + B) = A\,L(\chi) \tag{43}$$

for any tracer field χ and any constants A and B; (43) can conveniently be taken, in place of (16), as the definition of semi-linearity. The two most essential points are, first, that (43) is enough for the general argument below (18) still to hold, and, second, that the remaining arguments of section 6 hold likewise, with minor modifications, save for one class of exceptions consisting of cases of generalized slope equilibrium with strongly nonlinear functional relations $\chi(\psi)$. In practice the main difficulty is being sure whether a given semi-linear L is also invertible and homogenizing.

7.1. Numerical Simulation of Generalized Gradient Equilibrium

Consider first the case analyzed in section 6.1. Linearity of the transport operator was assumed in order to write equation (25), followed by invertibility to deduce (27). With semi-linearity in place of linearity, an extra step is required in the argument: first write $L(\chi) = L(\chi_0 + O(\varepsilon)) = L(\chi_0) + O(\varepsilon)$ (which requires only that $L(.)$ is independent of ε and behaves reasonably when $\varepsilon \to 0$ in its argument). Then (26) and (27) follow as before, separating powers of ε and assuming invertibility. That is, $L(\chi_0) = 0$ and χ_0 is independent of $\mathbf{x}$. Thus χ_0 can take the place of B in (43), so that $L(\chi) = \varepsilon L(\chi_1 + O(\varepsilon))$, and the rest of the argument follows. This confirms, as indicated more generally by (18)ff, that semi-linearity is enough to allow a numerical model to simulate PM's gradient equilibrium regime, if the model's transport scheme is also invertible and homogenizing.

The invertibility assumption is used twice in section 6.1: first, following (26), in the weak sense that the vanishing of $L(\chi)$ implies the vanishing of gradients of χ, and second, following (31), in the strong or general sense that the field χ is uniquely obtainable, apart from an undetermined additive constant, from the field $L(\chi)$ for any χ whatever. The strong and weak senses are equivalent for linear L—because for any $\chi^{(1)}$ and $\chi^{(2)}$ we have $L(\chi^{(1)}) = L(\chi^{(2)}) \Rightarrow L(\chi^{(1)} - \chi^{(2)}) = 0 \Rightarrow \chi^{(1)} - \chi^{(2)} = 0$—but not for nonlinear L. It was pointed out below (27) that non-invertible continuum transport operators L are possible in principle. The same goes for finite, numerical transport operators; indeed, they can fail to be even weakly invertible.

The linear advection scheme CD2 is the simplest example. On a regularly spaced one-dimensional grid with

a constant advecting wind, a tracer mixing ratio profile χ made up of a constant plus a two-grid wave of arbitrary but constant amplitude will give $L(\chi) = 0$, when L is the numerical transport operator defined by CD2 (details in Appendix A1). Thus CD2 fails to be invertible, both weakly and strongly, on, for example, a periodic domain with an even though not an odd number of grid points.

The invertibility or otherwise of VL2 and UL4 also depends on the domain in which they are considered. For the periodic domain, both VL2 and UL4 appear to be strongly as well as weakly invertible. This is indicated by numerical experimentation, and we have proven it explicitly for VL2 in the one-dimensional case (details omitted for brevity). In one-dimensional bounded domains with no boundary constraints on χ values, VL2 and UL4 are, by contrast, weakly but not strongly invertible. The reason why strong invertibility fails can be seen by considering a regular one-dimensional grid with a constant advecting wind and a tracer profile $\chi^{(1)}$ that has a uniform, nonvanishing gradient. For both VL2 and UL4 it is possible to find a different profile $\chi^{(2)} \neq \chi^{(1)}$ such that $L(\chi^{(2)}) = L(\chi^{(1)})$; this $\chi^{(2)}$ takes the form of a "worn staircase" profile, equal to $\chi^{(1)}$ plus a two-grid wave whose amplitude is restricted such that that the gradient of $\chi^{(2)}$ has the same sign everywhere as the gradient of $\chi^{(1)}$. For VL2 the two-grid wave amplifies in space, implying that the restriction to a finite domain is essential. For UL4 the two-grid wave has constant amplitude in space.

Also used in section 6 is the homogenization assumption, which, as already remarked, is logically distinct from assumptions about invertibility. CD2 provides a sufficient example, on a periodic domain with an odd number of grid points. It is then invertible but not homogenizing. So is the usual linear spectral advection scheme. Both it and CD2 fail to homogenize because both, as is well known, conserve total tracer variance. Note also that some transport operators may, in theory, homogenize, though extremely slowly. For example, with the VL2 scheme the square-wave χ and ψ distributions at the top left of Figures 4a,b do, in theory, homogenize, but only at a rate that is exponentially small in the number of grid points per wavelength, which may well become zero in practice because of roundoff error.

In practical numerical models, including GCMs, the model's transport operator—i.e., the advection scheme together with any other numerical operations such as scale-selective dissipation or filtering—must in any case, regardless of present concerns, be substantially homogenizing if the model is to have sensible-looking long term behavior. In GCM simulations the mixing ratio of an inert tracer tends to become homogenized throughout the model troposphere on a timescale of order 1 year [e.g., *Thuburn*, 1993].

Note in this connection that the CD2 scheme and the usual linear spectral advection scheme, neither of which are homogenizing, are widely used in GCMs for horizontal and vertical advection. When such advection schemes are used, therefore, homogenization must depend on adding extra, scale-selective dissipation terms to the model's transport operator in the usual way. From the foregoing remarks about VL2 and UL4, one may expect that flux-limited schemes will also, as a rule, require scale-selective dissipation to be added. The point then needing care is not to violate (43).

The general requirements are now clear for any numerical model intended to simulate the establishment, by transport, of linear correlations or functional relations between chemical species. The requirements apply to any circumstances covered by (18)ff., including gradient equilibrium regimes, and may be summarized by saying that, to guarantee the appropriate behavior, the model's transport operator $L(.)$ should be homogenizing, strongly invertible, and semi-linear (equation (43)). For this purpose $L(.)$ means the total transport operator, including the model's scale-selective or subgrid dissipation, as well as advective transport.

7.2. Numerical Simulation of Generalized Slope Equilibrium

The only circumstances not covered by the discussion just given are those outside the general scope of (18)ff., i.e., the cases of generalized slope equilibrium discussed in section 6.2 that lead to nonlinear functional relations $\chi = \chi(\psi)$. There, the assumptions were that the horizontal transport operator $H(.)$ satisfies the timescale separation (32) and is linear, homogenizing, invertible, and indifferent to vertical gradients—that is, able to see only the horizontal structure of the tracer field. Horizontal structure, for this purpose, has an unambiguous meaning, namely, structure on an isentropic surface, i.e., z = constant in the notation of section 6.2.

The timescale separation (32) and the indifference to vertical gradients have a straightforward meaning only in numerical models whose coordinate levels coincide with isentropic surfaces. In such a model we may usually isolate the horizontal part of the model's transport operator, and identify it with the $H(.)$ of section 6.2. As before, we can no longer expect the model's $H(.)$ to be linear, but if $H(.)$ is semi-linear, homogenizing, strongly invertible, and indifferent to vertical gradients, then the argument leading to (35) via (37) and (40) goes through exactly as before. In deriving (37), in particular, semi-linearity and indifference to vertical gradients means that the factor $\overline{\chi}_z$ can be treated like the constant A in (43), hence taken outside H^{-1} to give (37). Note that, for the reasons discussed in section 7.1, the vertical part of the model's transport scheme is likely to include, implicitly or explicitly, an extra scale-selective diffusion that will add to—and with present-day vertical resolutions may well be larger than—the K of equation (40). Otherwise, the model's vertical profiles will be vulnerable to problems like the two-grid-wave problem already discussed.

Models in coordinates other than isentropic will tend, in effect, to have still more vertical diffusion, from the indirect effect of mixing along sloping isentropes that cross the model's coordinate levels. With shallow slopes we can still have Fickian vertical diffusive behavior, for the reasons discussed in section 6.2. This may or may not be enough to prevent vertical two-grid waves, which have been found for instance in GCM simulations using scheme CD2 for vertical advection [e.g., *Thuburn*, 1993]. Such grid waves will cause spurious scatter in tracer correlation diagrams that would otherwise show linear functional relations $\chi(\psi)$, precisely because they imply failure of the invertibility and homogenization assumptions.

The timescale separation (32) between vertical and horizontal transport can be violated by "numerical mixing" (section 4.2). If $\chi(\psi)$ is strongly nonlinear, such that the two tracers have vertical profiles with very different height scales, then even a semi-linear, homogenizing, and strongly invertible model transport scheme will act differently on the two profiles, generally in such a way as to produce effects like those suggested in Figures 1a,b and discussed in section 4.2. These will be significant if and only if the "numerical mixing" is fast enough to compete strongly with the tendency toward generalized slope equilibrium.

8. Conclusions

In this paper we have addressed two closely related questions about numerical advection schemes, and about numerical transport schemes in general, namely, whether they can (*a*) preserve preexisting correlations or functional relations between the mixing ratios of different chemical species, and (*b*) establish such relations, as transport undoubtedly does for long-lived tracer species in the real atmosphere [PM, PK]. In the process, we have arrived at some general insights (sections 6,7) into when and how transport can have such effects both in the real atmosphere and in numerical models. Some of the theoretical results hold only in an ensemble-mean sense, and all can be interpreted in that sense, if desired, implying correlations with scatter rather than perfect functional relations.

Functional relations or correlations due to transport arise in two distinct ways. The first and most general way is characteristic of PM and PK's "gradient equilibrium" regimes and their generalizations, see (18)ff., and concerns linear relations only. The restriction to linear relations is essential to what is involved, namely, the shaping of two mixing-ratio fields "in the same way, making their isopleths coincide," in the fully general sense of (18)ff. An analogous shaping can occur in a numerical simulation whenever the model's transport operator $L(.)$ is semi-linear, homogenizing, and strongly invertible, as discussed in section 7.1. Note that the semi-linearity requirement, equation (43), excludes negative-value filling.

The second way is simply through the effects of fast transport on two-dimensional surfaces, as expressed by the timescale separation (32). This is characteristic of PK's stratospheric "slope equilibrium" regimes and their generalizations, see (35)–(41), in which the relevant surfaces are quasi-horizontal isentropes. Such transport will tend to produce one-dimensional mixing-ratio fields, implying that all species satisfying (32) are functionally related, perhaps nonlinearly. When (32) holds, the mixing-ratio isopleths have small but nonvanishing slopes relative to the isentropes; these slopes are the same for all species satisfying (32) and can depend on time and longitude as well as latitude, as is made explicit by equation (41). In order for a numerical model stratosphere to simulate such "generalized slope equilibrium" regimes, the most crucial requirements are that the horizontal transport operator $H(.)$ be homogenizing and strongly invertible, and that vertical "numerical mixing" (section 4.2) and any other vertical transport is slow enough not to violate (32), hence not to compete too strongly with the all-important fast horizontal transport.

All the foregoing requirements may well be satisfied, and satisfied rather easily, in a numerical model that is otherwise inaccurate. For instance the requirements for generalized gradient equilibrium seem practically certain to be satisfied if the model's transport operator is equivalent to any semi-linear advection scheme plus a sufficiently strong, and likewise semi-linear, or linear, scale-selective dissipation. Thus the successful preservation and establishment of linear functional relations and correlations, in particular, is no guarantee of model accuracy: shaping two tracer fields the same way does not imply shaping them the right way.

Appendix A: Advection Schemes

A1. Second-Order Centered Differences, CD2

Interfacial values $\chi_f = \chi_{k\pm1/2}$ of the mixing ratio, χ, on either side of the kth grid point are defined by

$$\chi_{k+1/2} = \tfrac{1}{2}(\chi_k + \chi_{k+1}) \tag{44}$$

and similarly for $\chi_{k-1/2}$. A leapfrog time step is used:

$$\chi_k^{(t+\Delta t)} = \chi_k^{(t-\Delta t)} - 2c\,(\chi_{k+1/2}^{(t)} - \chi_{k-1/2}^{(t)}) \tag{45}$$

where c is the Courant number,

$$c = u\,\Delta t/\Delta x \tag{46}$$

with u the wind speed, Δt the time step, and Δx the grid spacing, $\Delta x = x_{k+1} - x_k$.

A2. Flux-Limited Scheme VL2 Based on Second-Order Differences with the van Leer Limiter

Interfacial values $\chi_{k\pm1/2}^{\mathrm{H}}$ are defined on either side of the kth grid point in a way that corresponds to a high order, in this case second-order, scheme,

$$\chi^{\mathrm{H}}_{k+1/2} = (\chi_k + \chi_{k+1})/2 \tag{47}$$

and similarly for $\chi_{k-1/2}$. We also define interfacial values $\chi^{\mathrm{L}}_{k\pm1/2}$ that correspond to a low-order (first-order upwind) scheme, e.g.,

$$\chi^{\mathrm{L}}_{k+1/2} = \begin{cases} \chi_k, & c \geq 0 \\ \chi_{k+1}, & c < 0 \end{cases} \tag{48}$$

These are combined to give $\chi_{\mathrm{f}} = \chi_{k\pm1/2}$ where

$$\chi_{k+1/2} = \begin{cases} \chi^{\mathrm{L}}_{k+1/2} + \phi^+(r_k)(\chi^{\mathrm{H}}_{k+1/2} - \chi^{\mathrm{L}}_{k+1/2}), & c \geq 0 \\ \chi^{\mathrm{L}}_{k+1/2} + \phi^-(r_{k+1})(\chi^{\mathrm{H}}_{k+1/2} - \chi^{\mathrm{L}}_{k+1/2}), & c < 0 \end{cases} \tag{49}$$

and similarly for $\chi_{k-1/2}$. Here $\phi^{\pm}(r)$, the flux limiter, is defined by

$$\phi^+(r) = \frac{r + |r|}{1 + |r|}, \qquad \phi^-(r) = \phi^+(1/r) \tag{50}$$

where

$$r_k = \frac{\Delta\chi_{k-1/2}}{\Delta\chi_{k+1/2}} = \frac{\chi_k - \chi_{k-1}}{\chi_{k+1} - \chi_k} \tag{51}$$

A forward time step is used:

$$\chi^{(t+\Delta t)}_k = \chi^{(t)}_k - c(\chi^{(t)}_{k+1/2} - \chi^{(t)}_{k-1/2}) \tag{52}$$

Semi-linearity in the sense of (16) and (43) follows by noting that (51), being a ratio of differences, is independent of A and B when $\chi = A\psi + B$. Notice also that the flux limiter produces, among other effects, the nonlinear antidiffusive or step-steepening behavior mentioned in section 5.1. With $c > 0$, a step in mixing ratio separating two nearly flat regions, like that seen in the top left of Figure 4a, will have the flux limiter $\phi^+ > 1$ on the downwind side of the step and $\phi^+ < 1$ on the upwind side. Thus the scheme is biased downwind on the downwind side of the step and upwind on the upwind side, so that each grid point is most strongly influenced by the nearest nearly-flat region, and intermediate mixing ratios are prevented from diffusing outward.

A3. Flux-Limited Scheme UL4 Based on Fourth-Order Differences with the Universal Limiter

Interfacial values are defined corresponding to a high-order, in this case fourth-order, scheme,

$$\chi^{\mathrm{H}}_{k+1/2} = (-\chi_{k-1} + 7\chi_k + 7\chi_{k+1} - \chi_{k+2})/12 \tag{53}$$

and a low-order (first-order upwind) scheme (equation (48)). To get the interfacial values χ_{f}, the low-order value at time step $t - \Delta t$ is combined with the high-order value at time step t,

$$\chi^{(t-\Delta t,t)}_{k+1/2} = \begin{cases} \chi^{\mathrm{L}(t-\Delta t)}_{k+1/2} + \phi^+(\chi^{\mathrm{H}(t)}_{k+1/2} - \chi^{\mathrm{L}(t-\Delta t)}_{k+1/2}), & c \geq 0 \\ \chi^{\mathrm{L}(t-\Delta t)}_{k+1/2} + \phi^-(\chi^{\mathrm{H}(t)}_{k+1/2} - \chi^{\mathrm{L}(t-\Delta t)}_{k+1/2}), & c < 0 \end{cases} \tag{54}$$

where the flux limiter

$$\phi^+ = \max\left\{0, \min\left(\left(\frac{\Delta\chi^{(t-\Delta t)}_{k+1/2}}{\chi^{\mathrm{H}(t)}_{k+1/2} - \chi^{\mathrm{L}(t-\Delta t)}_{k+1/2}}\right), \left(\frac{1}{c} - 1\right)\left(\frac{\Delta\chi^{(t-\Delta t)}_{k-1/2}}{\chi^{\mathrm{H}(t)}_{k+1/2} - \chi^{\mathrm{L}(t-\Delta t)}_{k+1/2}}\right), 1\right)\right\} \tag{55}$$

$$\phi^- = \max\left\{0, \min\left(\left(\frac{-\Delta\chi^{(t-\Delta t)}_{k+1/2}}{\chi^{\mathrm{H}(t)}_{k+1/2} - \chi^{\mathrm{L}(t-\Delta t)}_{k+1/2}}\right), \left(\frac{1}{c} - 1\right)\left(\frac{-\Delta\chi^{(t-\Delta t)}_{k+3/2}}{\chi^{\mathrm{H}(t)}_{k+1/2} - \chi^{\mathrm{L}(t-\Delta t)}_{k+1/2}}\right), 1\right)\right\} \tag{56}$$

is equivalent to the "universal limiter" [*Leonard*, 1991; see also *Thuburn*, 1993]. Because the interfacial value depends on values at time step $t - \Delta t$ and time step t, the time step is a hybrid between forward and centered steps,

$$\chi^{(t+\Delta t)}_k = \chi^{(t-\Delta t)}_k - 2c(\chi^{(t-\Delta t,t)}_{k+1/2} - \chi^{(t-\Delta t,t)}_{k-1/2}) \tag{57}$$

where superscript $(t - \Delta t, t)$ means the average over the values at the two times. Semi-linearity in the sense of (16) and (43) follows by noting that (55) and (56), involving only ratios of differences, are independent of A and B when $\chi = A\psi + B$.

Appendix B: Monotone Schemes and "Numerical Mixing"

The following justifies the two assertions about monotone schemes made in section 4.2. We assume throughout that the advection scheme has property **4** of section 2, listed above equation (9), namely, that spatial homogeneity is preserved. Monotone, in the sense of *Harten* [1983], means that, at each time step $t \to t+\Delta t$, the scheme also satisfies

$$\partial\chi^{(t+\Delta t)}_{\mathsf{P}} / \partial\chi^{(t)}_{\mathsf{Q}} \geq 0 \tag{58}$$

for each pair of grid points P and Q (t and Δt being fixed while the grid point χ values vary).

First, this assumption implies, but is far more restrictive than, property **3** of section 2 that the scheme is shape preserving [*Harten*, 1983]. Property **3** is implied if we take extremum at the grid point P to mean the only thing that can be relevant, namely, an extremum with respect to every point of $\mathsf{S_P}$, the set of grid points seen by the scheme when updating the value at the grid point P. For instance, if the extremum is a maximum, with value $\chi^{(t)}_{\mathsf{P}} = \chi_{\max}$, say, at time t, then this is taken to mean that $\chi^{(t)}_{\mathsf{Q}} \leq \chi_{\max}$ at every point Q of $\mathsf{S_P}$. Then (58) implies that increasing all the $\chi^{(t)}_{\mathsf{Q}}$ values up to $\chi_{\max}$ would make $\chi^{(t+\Delta t)}_{\mathsf{P}}$ either increase or stay the same; and property **4** implies that the final

value of $\chi_{\mathsf{P}}^{(t+\Delta t)}$ would also have to be equal to $\chi_{\max}$. It follows that, with the actual $\chi_{\mathsf{Q}}^{(t)}$ values, $\chi_{\mathsf{P}}^{(t+\Delta t)} \le \chi_{\mathsf{P}}^{(t)}$. Similarly, if the extremum at P is a minimum, then $\chi_{\mathsf{P}}^{(t+\Delta t)} \ge \chi_{\mathsf{P}}^{(t)}$. This establishes property **3**.

The convex hull property, implying "numerical mixing" of a preexisting nonlinear functional relation to the concave side only, is established by extending the above reasoning as follows. Recall from section 4.2 that the convex hull of the set $I(\mathsf{S_P})$ is the smallest convex polygon enclosing all the points of $I(\mathsf{S_P})$, as illustrated in Figure 1b by the boat-shaped polygon AB...E. More generally, some of the points of $I(\mathsf{S_P})$ could be interior to the convex hull, which has the general property that each point of $I(\mathsf{S_P})$ lies either on the polygon, or to one side only, the interior side, of each straight line that makes up the polygon.

Consider one such straight line, say, L, extrapolated to infinity. It divides the $\psi\chi$ plane of the correlation diagram into exactly two parts, one of them containing all the points of $I(\mathsf{S_P})$. All these points can be moved on to L via parallel paths of finite slope, making all the values $\chi_{\mathsf{Q}}^{(t)}$ change in the same sense. So do all the corresponding values of ψ, say $\psi_{\mathsf{Q}}^{(t)}$. Furthermore, once all the points have been moved on to L, then the semi-linearity property (43) applies. This says that the corresponding updated values $\chi_{\mathsf{P}}^{(t+\Delta t)}, \psi_{\mathsf{P}}^{(t+\Delta t)}$ must also lie on L. Reversing the process and using (58) shows that the updated values from the actual $I(\mathsf{S_P})$ must lie on the same side of L as $I(\mathsf{S_P})$ itself. Repeating this argument for the other relevant straight lines of the convex hull shows that the updated values $\chi_{\mathsf{P}}^{(t+\Delta t)}, \psi_{\mathsf{P}}^{(t+\Delta t)}$ cannot lie outside the convex hull, as asserted.

Acknowledgments. We thank R. A. Plumb, L.C. Sparling, and two anonymous referees for their extremely valuable comments. The work was supported by the UK Natural Environment Research Council through the U.K. Universities' Global Atmospheric Modelling Programme and by the UK Engineering and Physical Sciences Research Council through a Senior Research Fellowship.

References

Allen, D.J., A.R. Douglass, R.B. Rood, and P.D. Guthrie, Application of a monotonic upstream-biased transport scheme to three-dimensional constituent transport calculations, *Mon. Weather Rev.*, *119*, 2456–2464, 1991.

Boering, K. A., et al., Stratospheric mean ages and transport rates from observations of carbon dioxide and nitrous oxide, *Science*, *274*, 1340–1343.

Boris. J.P., and D.L. Book, Flux corrected transport. I. SHASTA, a fluid transport algorithm that works, *J. Comput. Phys.*, *11*, 38–69, 1972.

Dewan, M.E., Turbulent vertical transport due to thin intermittent mixing layers in the stratosphere and other stable fluids, *Science*, *211*, 1041–1042, 1981.

Fahey, D.W., S. Solomon, S.R. Kawa, M. Loewenstein, J.R. Podolske, S.E. Strahan, and K.R. Chan, A diagnostic for denitrification in the winter polar stratospheres, *Nature*, *345*, 698–702, 1990.

Fiedler, B.H., An integral closure model for the vertical turbulent flux of a scalar in a mixed layer, *J. Atmos. Sci.*, *41*, 674–680, 1984.

Fiedler, B.H., and C.-H. Moeng, A practical integral closure model for mean vertical transport of a scalar in a convective boundary layer, *J. Atmos. Sci.*, *42*, 359–363, 1985.

Godunov, S.K., Finite difference method for numerical computation of discontinuous solutions of the equations of fluid dynamics (in Russian), *Mat. Sb.*, *47*, 271, 1959.

Harten, A., High resolution schemes for conservation laws, *J. Comput. Phys.*, *49*, 357–393, 1983.

Holton, J.R., A dynamically based transport parameterization for one-dimensional photochemical models of the stratosphere, *J. Geophys. Res.*, *91*, 2681–2686, 1986.

Lee, A.M., G.D. Carver, M.P. Chipperfield, and J.A. Pyle, Three-dimensional chemical forecasting: A methodology, *J. Geophys. Res.*, *102*, 3905–3919, 1997.

Leonard, B.P., The ULTIMATE conservative difference scheme applied to unsteady one-dimensional advection, *Comput. Methods Appl. Mech. Eng.*, *88*, 17–74, 1991.

Lin, S.-J., and R.B. Rood, Multidimensional flux-form semi-Lagrangian transport schemes, *Mon. Weather Rev.*, *124*, 2046–2070, 1996.

Mahlman, J.D., H. Levy II, and W.J. Moxim, Three-dimensional simulations of stratospheric N_2O: Predictions for other trace constituents, *J. Geophys. Res.*, *91*, 2687–2707, 1986.

McIntyre, M.E., Atmospheric dynamics: Some fundamentals, with observational implications, section 10, pp. 357ff. *Proceedings Int. School Phys. Enrico Fermi 115th Course*, ed. J. C. Gille, G. Visconti; North-Holland. 313–386, 1992.

Minschwaner, K., et al., The bulk properties of isentropic mixing into the tropics in the lower stratosphere, *J. Geophys. Res.*, *101*, 9433–9439, 1996.

Mote, P.W., et al., An atmospheric tape recorder: The imprint of tropical tropopause temperatures on stratospheric water vapor, *J. Geophys. Res.*, *101*, 3989–4006, 1996.

Pasquill, F., and F. Smith, *Atmospheric Diffusion*, pp. 141–158, John Wiley, New York, 1983.

Plumb, R.A., A "tropical pipe" model of stratospheric transport, *J. Geophys. Res.*, *101*, 3957–3972, 1996.

Plumb, R.A., and M.K.W. Ko, Interrelationships between mixing ratios of long-lived stratospheric constituents, *J. Geophys. Res.*, *97*, 10,145–10,156, 1992.

Plumb, R.A., and D.D. McConalogue, On the meridional structure of long-lived tropospheric constituents, *J. Geophys. Res.*, *93*, 15,897–15,913, 1988.

Prather, M.J., Numerical advection by conservation of second-order moments, *J. Geophys. Res.*, *91*, 6671–6681, 1986.

Proffitt, M.H., J.J. Margitan, K.K. Kelly, M. Loewenstein, J.R. Podolske, and K.R. Chan, Ozone loss in the Arctic polar vortex inferred from high-altitude aircraft measurements, *Nature*, *347*, 31–36, 1990.

Proffitt, M.H., S. Solomon, and M. Loewenstein, Comparison of 2-D model simulations of ozone and nitrous oxide at high latitudes with stratospheric measurements, *J. Geophys. Res.*, *97*, 939–944, 1992.

Slingo, J., M. Blackburn, A. Betts, R. Brugge, K. Hodges, B. Hoskins, M. Miller, L. Steenman-Clark, and J. Thuburn, Mean climate and transience in the tropics of the UGAMP GCM: Sensitivity to convective parametrization. *Q. J. R. Meteorol. Soc.*, *120*, 881–922, 1994.

Stull, R.B., Transilient turbulence theory, I: The concept of eddy mixing across finite distances, *J. Atmos. Sci.*, *41*, 3351–3367, 1984.

Sweby, P.K., High resolution TVD schemes using flux limiters, *Lect. Appl. Math.*, *22*, 289–309, 1985.

Taylor, G.I., Diffusion by continuous movements, *Proc. London Math. Soc. Ser. 2*, *20*, 196–212, 1921.

Taylor, G.I., Dispersion of soluble matter in solvent flowing slowly through a tube. *Proc. R. Soc. London A, 219*, 186–203, 1953.

Thuburn, J., Use of a flux limited scheme for vertical advection in a GCM, *Q. J. R. Meteorol. Soc., 119*, 469–487, 1993.

Thuburn, J., Dissipation and cascades to small scales in numerical models using a shape-preserving advection scheme, *Mon. Weather Rev., 123*, 1888–1903, 1995.

Thuburn, J., Multidimensional flux-limited advection schemes, *J. Comput. Phys., 123*, 74–83, 1996.

Van Leer, B., Towards the ultimate conservative difference scheme, II, Monotonicity and conservation combined in a second order scheme, *J. Comput. Phys., 14*, 361–370, 1974.

Volk, C.M., et al., Quantifying transport between the tropical and midlatitude lower stratosphere, *Science, 272*, 1763–1768, 1996.

Waugh, D.W., et al., Mixing of polar vortex air into middle latitudes as revealed by tracer-tracer scatterplots. *J. Geophys. Res.* in press, 1996.

Zalesak, S.T., Fully multidimensional flux corrected transport algorithms for fluids, *J. Comput. Phys., 31*, 335–362, 1979.

J. Thuburn, Centre for Global Atmospheric Modelling, Department of Meteorology, Reading University, Reading, RG6 6BB, England. (e-mail: swsthubn@met.reading.ac.uk; http://typhoon.rdg.ac.uk/ugamp/ugamp.html)

M.E. McIntyre, Centre for Atmospheric Science at the Department of Applied Mathematics and Theoretical Physics, University of Cambridge, Silver Street, Cambridge, CB3 9EW, England. (e-mail: mem@damtp.cam.ac.uk; http://www.atmos-dynamics.damtp.cam.ac.uk)

(Received September 28, 1995; revised October 30, 1996; accepted October 30, 1996.)